

Binary stars in young clusters: models versus observations of the Trapezium Cluster

Pavel Kroupa¹, Monika G. Petr^{2,4}, and Mark J. McCaughrean³

¹Institut für Theoretische Astrophysik, Universität Heidelberg, Tiergartenstr. 15, D-69121 Heidelberg, Germany
e-mail: pavel@ita.uni-heidelberg.de

²Max-Planck-Institut für Astronomie, Königstuhl 17, D-69117 Heidelberg
e-mail: mpetr@eso.org

³ Astrophysikalisches Institut Potsdam, An der Sternwarte 16, D-14482 Potsdam, Germany
e-mail: mjm@aip.de

Summary

The frequency of low-mass pre-main sequence binary systems is significantly lower in the Trapezium Cluster than in Taurus-Auriga. We investigate if this difference can be explained through stellar encounters in dense clusters. To this effect, a range of possible models of the well observed Trapezium Cluster are calculated using Aarseth's direct N-body code, which treats binaries accurately. The results are confronted with observational constraints. The range of models include clusters in virial equilibrium, expanding clusters as a result of instantaneous mass loss, as well as collapsing clusters. In all cases the primordial binary proportion is larger than 50 per cent, with initial period distributions as observed in Taurus-Auriga and the Galactic field.

It is found that the expanding model, with an initial binary population as in the Galactic field, is most consistent with the observational constraints. This raises the possibility that the primordial group of OB stars may have expelled the cluster gas roughly 50 000 yr ago. The cluster's bulk expansion rate is thus a key observable that needs to be determined. The other models demonstrate that the rapidly decreasing binary proportion, its radial dependence and the form of the period distribution, together with structural and kinematical data, are very useful diagnostics on the present and past dynamical state of a young cluster. In particular, kinematical cooling from the disruption of wide binaries is seen for the first time.

PACS: 98.10.+z; 98.20.-d; 97.80.-d; 97.10.Bt

Subject headings: stars: binaries: general – stars: formation – open clusters and associations: individual (Trapezium Cluster, M42)

1. INTRODUCTION

To develop an improved understanding of star formation it is very useful to empirically map variations of the binary-star properties and the initial mass function with environment, such as metallicity, density and

⁴present address: European Southern Observatory, Casilla 19001, Santiago 19, Chile

temperature of the star-forming cloud. However, a naive interpretation of observational data may result in misleading conclusions. For instance, a comparison of binary proportions in different stellar populations, without taking into account the dynamical history of the population, is ill-fated, because the distribution of orbital elements of a population carries a memory of the dynamical history (Kroupa 1998). One purpose of this paper is to further illustrate, on the one hand this danger, and on the other hand, the richness in understanding that can be gained through stellar-dynamical studies of young stellar systems.

The Trapezium Cluster in the Orion star forming region is a young, populous stellar cluster, which contains a negligible amount ($< 10 M_{\odot}$) of residual gas (Wilson et al. 1997; O’Dell 1999, private communication) and for which a large amount of observational data has been collected over decades. Thus, it is an excellent target for investigating the early dynamical evolution of a young cluster with a primordial binary proportion at least as large as in the Galactic field. The cluster’s age is estimated to be younger than 5 Myr (Prosser et al. 1994; Hillenbrand 1997), and probably $\lesssim 10^6$ yr. The central stellar number density is very high, with the mean inter-stellar separation being about 6000 AU (McCaughrean & Stauffer 1994). The Trapezium Cluster is a well-suited sample for the study of star formation in a dense stellar environment, as opposed to the low-density young stellar groups in the Taurus-Auriga star forming region (Gomez et al. 1993; Briceno et al. 1998).

Variations in stellar properties may occur with star formation environment. For example, the observed pre-main sequence binary population in the Trapezium Cluster is significantly different than in Taurus-Auriga. In the latter approximately all stars are in binary systems (Köhler & Leinert 1998; Duchene 1999; Ghez et al. 1997), while in the Trapezium Cluster the binary proportion is significantly lower (Prosser et al. 1994; Petr 1998; Petr et al. 1998; but see also Padgett, Strom & Ghez 1997), being comparable to what is found in the Galactic field (Duquennoy & Mayor 1991). This, however, does not necessarily imply that most Galactic field stars stem from Trapezium-Cluster type assemblages, there being evidence that the proportion of long-period binary systems is significantly below the Galactic field value (Scally, Clarke & McCaughrean, 1999). The binary population may well decrease further in the Trapezium Cluster, if it is a bound entity. And it may have been higher at birth.

A stellar system with a half-mass radius of $R_{0.5} = 0.1 - 0.3$ pc, containing $N = 1000 - 2000$ stars, with a mass $M_{cl} = 300 - 600 M_{\odot}$, has a relaxation time $t_{relax} = 0.6 - 4.2$ Myr, which is the time-scale over which the cluster loses memory of its initial conditions. These are characteristic observed values for the Trapezium Cluster. The three-dimensional velocity dispersion in the Trapezium Cluster is $\sigma \approx 4.3$ km/s, the crossing time being $t_{cross} = 2 - 7 \times 10^4$ yr (an overview of the dynamical evolution of young clusters can be found in Bonnell & Kroupa 1999). A typical star may thus have crossed the central region many times, given that the age of the cluster is $\lesssim 1$ Myr. This implies that collisions between stellar systems will have been frequent. It also implies that the birth structure of the cluster will have been eradicated. Indications that this may be the case comes from the apparent lack of sub-structure (Bate, Clarke & McCaughrean 1998).

The Trapezium Cluster may thus be just old enough to perhaps have allowed an initial Taurus-Auriga binary population to have dynamically evolved to the observed reduced value. Alternatively, it may well be true that the lower binary proportion of the Trapezium Cluster as compared to the Taurus-Auriga star forming region is due to different star-forming conditions. Durisen & Sterzik (1994) point out that binary formation from fragmentation of collapsing and rotating clouds, or from a gravitational instability of massive proto-stellar disks, is more likely in low-temperature clouds.

That the binary proportion is eroded efficiently in a dense cluster has been shown by Kroupa (1995a).

However, whether the observed difference between the Trapezium Cluster and Taurus-Auriga can be explained with this mechanism must be investigated by constructing self-consistent models, that more closely match the properties of the Trapezium Cluster. If such a study shows that encounters are not efficient enough for a wide variety of models of the Trapezium Cluster, then the conclusion must be that the binary proportion depends on star-forming conditions. The aim of this paper is to begin tackling this problem by comparing evolving model populations with the constraints given by observations.

In this paper we present the first steps towards more realistic fully self-consistent models of embedded clusters in general, and of the Trapezium Cluster in particular. Section 2 summarises the available observational constraints and Section 3 details the model assumptions. In Section 4 we explain the calculation and data-evaluation programmes. The results are presented in Section 5, and Sections 6 and 7 contain the discussion and conclusions, respectively. An accompanying paper (Kroupa 1999) generalises these results to different numbers of stars and cluster radii, with a view to discussing the dynamical state of the Orion Nebula Cluster and the set of viable initial conditions.

2. OBSERVATIONAL CONSTRAINTS

The aim of this investigation is to study the evolution of those observables that allow the dynamical state of a young cluster and its birth configuration to be constrained. Such observables are the velocity dispersion, the central stellar volume number density and the radial dependence of the binary proportion.

2.1. Total number of stars, cluster age, and central density

In an optical high-resolution study carried out with the Hubble Space Telescope, 319 stars in a region with size $\sim 0.45 \text{ pc} \times 0.45 \text{ pc}$ were identified (Prosser et al. 1994). In a near infrared study covering a field of $\sim 5' \times 5'$ ($\sim 0.65 \text{ pc} \times 0.65 \text{ pc}$) centred on the Trapezium Cluster, McCaughrean et al. (1996) counted 700 systems (we call a single as well as a binary star a system). Binary stars with separations below the 0.7 arcsec seeing limit were not resolved. This corresponds to a resolution limit of $\approx 314 \text{ AU}$, or $\log_{10} P \approx 6.3$, where P is in days, for a system with a mass of $1 M_{\odot}$.

A high-spatial-resolution direct-imaging near-infrared study revealed even more stars in the innermost centre of the Trapezium Cluster (McCaughrean & Stauffer 1994), and a remarkably high stellar density of $\sim 5 \times 10^4$ stars per pc^3 was estimated. McCaughrean & Stauffer (1994) calculated that 29 systems are within the central spherical volume with a radius of $R = 0.053 \text{ pc}$.

From the analysis of the HR-Diagram, based on optical photometry and spectroscopy, Hillenbrand (1997) derived a mean age for the whole Orion Nebula Cluster less than 1 Myr, with an age spread of a few Myr. The age determination given by Prosser et al. (1994) is limited to the stars associated with the Trapezium Cluster and led to a medium age of $\sim 3 \times 10^5 \text{ yr}$, with nearly no detectable age spread.

2.2. Velocity dispersion, σ_{op}

The projected one-dimensional velocity dispersion in the observational plane, within $r = 0.41 \text{ pc}$ of the centre of the Trapezium Cluster, was derived by Jones & Walker (1988) to be $2.54 \pm 0.27 \text{ km/s}$ from their

proper-motion survey using photographic plates. The data indicate no anisotropy, but these authors, van Altena et al. (1988) and Tian et al. (1996) note that the plate-reduction algorithms eliminate any signature due to rotation and/or expansion or contraction. Thus, it is presently unknown if the Trapezium Cluster is expanding or contracting. The analysis of new absolute proper motions of a few dozen stars in the inner region ($\lesssim 2.5$ pc) of the Orion Nebula Cluster (ONC), of which the Trapezium Cluster is likely to be merely the central part, however, suggests that there may be some expanding motion (Frink, Kroupa & Röser 1999). For the present analysis we adopt the velocity dispersion obtained from the more precise relative proper motions, which we take to be corrected for radial bulk motions.

Photographic plates have a spatial resolution of typically 2 arcsec, which corresponds to about 1000 AU in the Trapezium Cluster. Most binary systems are therefore not resolved in these surveys.

2.3. Binary proportion

Observations using the speckle holography technique in the core of the Trapezium Cluster by Petr et al. (1998) resolve binary systems with separations in the range $d_1 = 63$ AU to $d_2 = 225$ AU. Of the 42 systems that appear projected within the central radius, $r = 0.041$ pc, six are OB stars and four are binary systems within the studied range of separations. The apparent binary proportion of the entire sample is $f_{\text{app}} = 0.095 \pm 0.05$ (equation 3 below), and the binary proportion for low-mass ($m < 1.5 M_{\odot}$) stars is $f_{\text{app,lms}} = 0.06 \pm 0.04$. The subscript “app” means that the observed f is the apparent binary proportion that an observer deduces from projected star positions within some range of separations to which the observational apparatus is sensitive. The binary proportion of low-mass stars within the central radius $r = 0.25$ pc is found by Prosser et al. (1994) using HST imaging to be $f_{\text{app}} = 0.12 \pm 0.02$ in the separation range $d_1 = 26$ AU to $d_2 = 440$ AU. The orbital periods corresponding to the respective separations are given in Fig. 3.

Both studies thus find a binary proportion, in the respective distance ranges sampled, that is similar to the Galactic field value, implying no measurable radial dependence of f for $r < 0.3$ pc (for details see Prosser et al. 1994, and Petr et al. 1998).

3. MODEL CLUSTERS

In this section we construct the model clusters. The appearance of the Trapezium Cluster today does not reflect the initial conditions when the stars decoupled dynamically from the gas, because the velocity dispersion of 2.5 pc/Myr implies significant mixing or spreading within 0.5–1 Myr. We therefore realize a variety of initial dynamical states. These cover models in cold collapse through initially virialised systems to clusters that expand.

3.1. The stellar population

The following parameters are chosen to specify possible different model Trapezium Clusters at “birth”, i.e. at the time when stellar dynamics starts dominating over gas dynamics:

- $N = 1600$ stars (point masses);

- The initial mass function (IMF) deduced from a careful analysis of star-count data in the Galactic field (Kroupa, Tout & Gilmore 1993) with power-law index $\alpha_1 = 1.3$ for $m \leq 0.5 M_\odot$; this IMF is based on Scalo’s (1986) IMF for stars with $m > 1 M_\odot$;
- Lower and upper stellar mass limits of $m_l = 0.08 M_\odot$ and $m_u = 30 M_\odot$, respectively;
- A Plummer density distribution (Aarseth, Henon & Wielen 1974);
- The initial position and velocity vectors of the binary-star centre-of-masses and single stars are independent of stellar mass;
- The velocity distribution of the binary centre-of-masses and single stars is isotropic.

Models in virial equilibrium (A1, A2), expanding models (B1, B2) and two cases of a cold collapse (models C1 and C2) are computed. Details of the models are given in Table 1, the entries of which are described below and in the following sub-sections.

The resulting cluster mass is $M_{cl} = 700 M_\odot$. The models contain no gas mass. This is a safe assumption because Wilson et al. (1997) and C.R. O’Dell (private communication) estimate the mass of gas to be only a few M_\odot in the Trapezium Cluster. The choice of the initial number of stars is guided by the evidence presented in Section 2.1, remembering that not all Trapezium Cluster stars will have been detected, as binary systems are usually not resolved in lower spatial resolution imaging studies. A binary proportion of 60 per cent implies $N = 1120$ stars. However, we choose $N = 1600$ since rapid reduction of the number of systems in the observed area ($0.65 \times 0.65 \text{ pc}^2$) is to be expected owing to expansion of the cluster and ejection of stars. Severe computational complications are avoided by assuming the stars have no extent. The assumption that the velocity and position vectors are not correlated with the stellar mass contradicts the observations, which show that the massive stars are concentrated in the cluster core. However, the present assumption allows investigation of whether dynamical mass-segregation in young binary-rich clusters can lead to the observed mass-segregation on time-scales of 1 Myr or less. This will be the subject of another paper. The initial placement of the massive stars in the present models is also consistent with the empirical finding that ultra-compact HII regions in areas of rich and active star formation are usually distributed throughout the region over spatial scales of about 1 pc (e.g. Megeath et al. 1996).

3.2. Initial dynamical state

The initial half-mass radius, $R_{0.5}$, is listed in column 2 of Table 1. For models A1 to B2 it is based on the results of McCaughrean & Stauffer (1994). Columns 3 and 4 list, respectively, the number of systems and stars within the central radius $R = 0.053 \text{ pc}$, and the central density ($\rho_c = 3N/[4\pi(0.77R_{0.5})^3]$, where $0.77R_{0.5}$ is the Plummer radius) is given in column 5. The parameters for models A1 and A2 are a compromise in that they give a central density that is larger by an order of magnitude than the observed value, and a velocity dispersion that is somewhat smaller than the observed value for virial equilibrium. The central density corresponds to an inter-system spacing of 2200 AU. In this case, the initial model median relaxation and half-mass diameter crossing times are $t_{relax} = 0.62 \text{ Myr}$ and $t_{cross} = 0.059 \text{ Myr}$, respectively. The central number density decreases and the half-mass radius increases within about 10^6 yr owing to mass segregation and associated expansion, and heating through binary stars. The precise evolution cannot be anticipated though, because it is not possible to easily estimate the various channels of energy exchange that exist in such a complex gravitational system, and since such realistic computations have never been performed heretofore.

Column 6 of Table 1 contains the initial virial ratio, $Q = E_{kin}/|E_{pot}|$, where the nominator and

denominator are, respectively, the total kinetic and potential energy of the whole cluster ($E_{\text{kin}} = 0.5 \sigma^2 M_{\text{cl}}$ and $E_{\text{pot}} = -G M_{\text{cl}}^2 / R_{\text{G}}$, where M_{cl} is the cluster mass, σ is the three-dimensional velocity dispersion, R_{G} is a characteristic cluster radius, and G is the gravitational constant). One possible state is virial equilibrium, $Q_{\text{v}} = 0.5$. However, the cluster may be expanding or contracting (see Section 2.2). To cover such possibilities, cluster models in virial equilibrium, expanding ($Q_{\text{exp}} = 1.2$) and cold collapse ($Q_{\text{col}} = 0.01$) are studied.

If the total cluster mass before mass loss is M_{tot} , and if the cluster is initially in virial equilibrium, then for a sudden mass loss of amount M_{gas} , the new

$$Q_{\text{exp}} = \frac{Q_{\text{v}}}{1 - M_{\text{gas}}/M_{\text{tot}}} = \frac{Q_{\text{v}}}{\epsilon}, \quad (1)$$

where $\epsilon = M_{\text{cl}}/M_{\text{tot}}$ is the star-formation efficiency. Assuming the cluster instantly loses a mass $M_{\text{gas}} = 0.58 M_{\text{tot}}$ ($\epsilon = 0.42$), $Q_{\text{exp}} = 1.2$, and the velocities are larger by a factor of $(Q_{\text{exp}}/Q_{\text{v}})^{1/2} = \epsilon^{-1/2} = 1.55$ than in a cluster in virial equilibrium with a mass $M_{\text{cl}} = M_{\text{tot}} - M_{\text{gas}} = 0.42 M_{\text{tot}}$. Thus, in the case of the expanding models (B1, B2), the initial velocities are increased by a factor of 1.55. These models assume that the massive stars have driven out a gas mass, $M_{\text{gas}} = 967 M_{\odot}$, immediately after they “turn on”, which is the time when the stellar-dynamical computation begins ($t = 0$). This mass loss corresponds to a rather high star-formation efficiency of 42 per cent, which is nevertheless expected to lead to an expanding, unbound association (Lada, Margulis & Dearborn 1984). It is also in-line with the masses of outflows observed around young OB stars which have short ($\lesssim 10^4$ yr) durations (Churchwell 1997). In such models it is possible that most of the cluster existed in an embedded phase for a few 10^5 yr before the hypothetical gas expulsion event. This phase, however, is not modelled here.

Models C1 and C2 are clusters which undergo cold collapse from two different initial $R_{0.5}$. To achieve this, the initial velocities of all binary centre-of-masses and single stars are multiplied by a factor $(Q_{\text{col}}/Q_{\text{v}})^{1/2} = 0.14$ (zero initial velocities are problematical for the N-body programme and would also be unrealistic since some clump–clump motions will always be present in the proto-cluster). Such models are interesting because dynamical friction on dense gas clumps moving in an extended gas medium is expected to lead to the contraction of a proto-cluster (Saiyadpour, Deiss & Kegel 1997; Ostriker 1999). Furthermore, relative ammonia-clump– C^{18}O -core velocities in larger (by a factor of 2–3) C^{18}O cores are often observed to be significantly smaller (≈ 0.1 km/sec) than the observed velocity dispersion (≈ 0.5 km/s) of the core, which is thought to be close to the virial value of the core (fig. 45 in Benson & Myers 1989). In this picture, individual stellar systems remain trapped in the potential wells locally dominated by the clumps that formed them, until most of the gas is removed. Clearly, relative clump–clump velocities need to be measured for cores containing many clumps, to verify if this picture is correct. Finally, the proper motion measurements within the Trapezium Cluster (Section 2.2) cannot exclude a model in which the cluster is collapsing, or is in the phase of violent relaxation (Lynden-Bell 1967) after a cold collapse.

3.3. Primordial binary systems

For each model cluster different assumptions concerning the primordial binary star population are made. In Table 1, column 7 lists the primordial total binary proportion,

$$f_{\text{tot}} = \frac{N_{\text{bin}}}{N_{\text{bin}} + N_{\text{sing}}}, \quad (2)$$

where N_{sing} and N_{bin} are the numbers of single-star and bound-binary systems, respectively. Column 8 contains the maximum binary-star period. The minimum period is $P_{\text{min}} = 1$ day in all cases. The form of the primordial period distribution is defined in column 9, where K2 refers to the eigenevolved (see below) birth distribution, which is consistent with young systems in Taurus–Auriga, and DM91 (Duquennoy & Mayor 1991) refers to the Gaussian log-period distribution approximating the distribution of systems in the Galactic field. A $1 M_{\odot}$ system has, with $\log_{10} P_{\text{max}} = 8.43$ (11.0) a semi-major axis of 8200 AU (4.2×10^5 AU). The model period distributions are compared with the observational data in Fig. 1. Note that the *primordial* f_{tot} is immediately reduced to the *initial* f_{tot} owing to disruptive crowding, which means through the immediate non-dynamical ionization of long-period binaries owing to their overlap in the high-density central region of the cluster.

With $f_{\text{tot}} = 1$, the assumption is made that the binary-star properties do not vary with star-forming conditions, apart from the effects of crowding, and that they are identical for the Trapezium Cluster to what is observed in Taurus–Auriga. With $f_{\text{tot}} = 0.6$, the hypothesis is that the binary proportion is lower in higher temperature star-forming clouds (Durisen & Sterzik 1994).

Additionally, the following assumptions are made:

- The primordial mass-ratio distribution is obtained by random pairing of the stars.
- The primordial eccentricity distribution is thermally relaxed.

The first assumption implies a mass-ratio distribution for G-dwarf systems that increases steeply towards low-mass secondaries. However, in the Galactic field (Duquennoy & Mayor 1991), the mass-ratio distribution for G-dwarf binary systems contains fewer M dwarf companions than the initial model here. The assumption and Galactic-field distribution are consistent with each other, because dynamical interactions in clusters can explain the observed properties of binary stars in the Galactic field, this being part of the *inverse dynamical population synthesis* argument for a clustered origin of most stars (Kroupa 1995a, 1995b). The available observational evidence on the mass-ratio distribution of very young stars is also consistent with the assumption of random-pairing from the IMF (Leinert et al. 1993).

The second assumption is necessary, because dynamical interactions in a Galactic cluster cannot evolve an arbitrary initial eccentricity distribution to the thermal distribution observed for main sequence binary systems with $\log_{10} P \gtrsim 3$, in which the number of systems increases linearly with the eccentricity. The primordial distribution is, however, evolved prior to the start of the N -body integration to account for *pre-main sequence eigenevolution* (i.e. the changes in orbital parameters owing to processes internal to a binary system such as tidal circularisation during the pre-main sequence phase). Only binary systems with $\log_{10} P \lesssim 3$ are affected by this. Details can be found in Kroupa (1995b).

4. THE N-BODY PROGRAMME AND DATA ANALYSIS

4.1. Aarseth’s NBODY5

The computation of the dynamical evolution of star clusters is expensive because the forces have to be calculated for each pair of stars so that the CPU time scales as N^2 . Binary systems that are perturbed by neighbours, and thus need to be integrated with very small time-steps, cause additional serious bottlenecks. An N -body programme must be able to handle dynamical processes that have time-scales ranging from

days to many 10^8 yr. The state-of-the art programmes for the dynamical modelling of star clusters on commercially available personal computers have been developed by Aarseth (1985, 1994, 1999).

For the present investigation, the successful and well tried NBODY5 programme is used. It incorporates many special algorithms to ensure computational speed and efficiency. Each particle is advanced with its own time-step, and the accelerations acting on it are updated with different frequencies using different techniques, depending on whether the perturbing stars are in a near-neighbour list or if the forces stem from numerous distant cluster members. Binary, triple and higher order systems are treated with the regularisation technique which, with a special transformation of space-time coordinates, eliminates the time-step singularity for closely interacting stars (see Aarseth 1999 for the state-of-the art).

The version of NBODY5 employed here has been used earlier for the calculation of the dynamical evolution of binary-rich clusters by Kroupa (1995a,b,c). It has extra routines that allow the inclusion of binary star populations with a variety of different initial period and eccentricity distributions. Position and velocity vectors of each star are output at regular time intervals, and form the basic data from which all binary star properties are derived in subsequent data analysis.

While statistical results from N -body calculations correctly describe the overall dynamical evolution, the velocity and position vectors of any individual centre-of-mass particle (e.g. a star or binary system) diverge exponentially from the true trajectory, through the growth of errors in N -body computations. Goodman, Heggie & Hut (1993) discuss these issues in depth. $N_{\text{run}} = 3$ computations with different initial random number seeds are performed for each model discussed here, giving in total 18 N -body calculations. All quantities inferred from the models and presented here are averages from three models. The computations are performed for a time-span of 5 Myr only, which is the upper limit for the age of the Trapezium Cluster from HR-diagram fitting (Hillenbrand 1997), although the mean age is probably closer to 1 Myr. Mass loss through stellar evolution can thus be neglected.

4.2. Data evaluation programme

An elaborate data-reduction programme reads the output from NBODY5 and calculates, among many quantities, the projected velocity dispersion, the number of bound binary systems and their properties. The observational plane is taken to be the $y - z$ plane, with the z direction being perpendicular to the Galactic disk. Throughout this paper, r refers to the projected radial distance from the density maximum, whereas R refers to the 3D distance. The choice of the projection plane is inconsequential for the present analysis, because r is always smaller than a few pc.

The apparent binary proportion,

$$f_{\text{app}} = \frac{N_{\text{app,bin}}}{N_{\text{app,bin}} + N_{\text{app,sing}}}, \quad (3)$$

a hypothetical observer located at infinity sees in the projected data, is calculated from the projected positions of all stars seen within a central circle with radius r in one model cluster at time t . The number, $N_{\text{app,bin}}$, of apparent stellar pairs with separations in the distance range d_1 to d_2 are counted together with the number of apparently single stars, $N_{\text{app,sing}}$. Binary systems with a separation $d < d_1$ are counted as single stars, and binary systems with $d > d_2$ are counted as two single stars. This is done for all stars within a central radius r .

For a comparison with proper motion data, the one-dimensional velocity dispersion of centres-of-masses

(i.e. unresolved stellar systems) in the observational plane, σ_{op} is calculated within some r . For consistency with the observational data, σ_{op} is corrected for the bulk radial motion giving $\sigma_{\text{op},c}$. To this end, the mean projected radial velocity, $\langle v_r \rangle$, within r is calculated. The corresponding radial vector quantity is subtracted from each 2D velocity vector. In the equilibrium models (A), $\langle v_r \rangle \approx 0$, while for the expanding models (B), $\langle v_r \rangle > 0$, and for the cold collapse models (C), $\langle v_r \rangle < 0$, for $t > 0$. The bulk radial motion is zero at $t = 0$ in the equilibrium and expanding models, because the velocity vectors are initially isotropically distributed.

5. RESULTS

In this section the results are described for each model (virial equilibrium, expansion and cold collapse) in turn. The overall cluster evolution and the evolution of the binary star population, as seen by a hypothetical observer, are discussed in separate subsections. Throughout the discussion the binary-star orbital period is used instead of the binding energy, which is $e_b = -P^{-2/3} \left[m_1 m_2 / (m_1 + m_2)^{1/3} \right] G/2$, where m_1 and m_2 are the component masses, and G is the gravitational constant in appropriate units. A detailed theoretical treatment of energy exchanges of binary systems with field stars is given by Heggie (1975).

5.1. Clusters in virial equilibrium – A

5.1.1. Cluster evolution

The models are initially over-dense by an order of magnitude (Fig. 2), but the central system density agrees with the observational constraint after 2.3 Myr (model A2) and 4.2 Myr (model A1). The cluster expands mostly through three- and four-body interactions. In a cluster consisting initially of single stars, on the other hand, the central number density would increase continuously until core collapse (e.g. Heggie & Aarseth 1992; Spurzem & Takahashi 1995). That the number of systems is consistently higher in model A1 than in model A2 for $t > 0.5$ Myr is a result of enhanced binary destruction in model A1, which contains a larger number of binaries with long periods. The disruption of wide binaries cools cluster A1, which expands more slowly than cluster A2, leading to a larger density in the core.

The one-dimensional velocity dispersion (Fig. 2) is similar to the observed value for $t \lesssim 0.5$ Myr, but then decreases substantially. The velocity dispersion is significantly smaller than the observational constraint when the central number density agrees with the observations. The higher density leads to a higher velocity dispersion in model A1. This is a manifestation of the negative specific heat capacity of gravitating systems: cooling implying a hotter system (Lynden-Bell 1998; see also Bonnell & Kroupa 1999).

In both models A1 and A2, the mean projected radial velocity, $\langle v_r \rangle \approx +0.08$ km/s for $t \lesssim 2$ Myr, testifying to the expansion noted above. At later times $\langle v_r \rangle \approx +0.05$ km/s, which corresponds to the smaller rate of decrease of the central number density evident in the upper panel of Fig. 2 after 2.2 Myr. This is linked to the end of the main destruction phase of long-period binary systems. The small radial bulk motion, $\langle v_r \rangle$, has a negligible effect on the observed velocity dispersion ($\sigma_{\text{op},c}$).

The change in slope in the upper panel of Fig. 2 at $t \approx 2.2$ Myr comes about because binary destruction moves the truncation of the period distribution to decreasing periods and thus towards the hard/soft binary boundary (see Fig. 1). Meanwhile binary activity (i.e. the energy exchange between the binary systems

and the cluster field) expands the cluster, causing a shift of the hard/soft boundary to longer periods. Ultimately, at time t_t further binary destruction is effectively halted, at which stage the hard/soft boundary has moved beyond the truncation period of the period distribution, which in turn implies a reduction of heating of the cluster field by hardening binaries. The hard/soft, or *thermal*, boundary corresponds at this stage to $P_{\text{th}} = 10^{6.0}$ days, taking the three-dimensional velocity dispersion $\sigma = \sqrt{3}\sigma_{\text{op,c}} = 2.1$ km/s to be the circular velocity of a system with a total mass of $1 M_{\odot}$. Thus, at $t > t_t \approx 2.2$ Myr the cluster retains an approximately constant density, an equilibrium state between the remaining binary population and the cluster field having been established.

5.1.2. The binary stars

The theoretical apparent projected binary star proportion, f_{app} , is compared with observational constraints in Fig. 3. Significant evolution of f_{app} occurs within the first 1 Myr, owing to disruption of binaries and diminishing number of chance projection pairs as the cluster expands. However, $f_{\text{app}}^{\text{modelA1}} > f_{\text{app}}^{\text{modelA2}}$ for $t < 4.2$ Myr in the upper panel, suggesting that the initial binary proportion and period distribution can, in principle, be constrained. The above inequality is violated for times $t > 1$ Myr in the much smaller sample in the cluster core, and information on the initial binary proportion is lost. The model results show that the observational constraints are still too weak to allow a distinction between models A1 and A2. Both are consistent with the data for dynamical cluster ages $t \gtrsim 0.3$ Myr.

The total binary proportion, f_{tot} (equation 2), also shown in Fig. 3, decreases rapidly for $t \lesssim 0.5$ Myr, and later at a much slower rate. At $t = 0$, f_{tot} is lower than the assumed primordial proportions because wide binary systems are disrupted through superposition in the crowded inner cluster region (see Section. 3.3). That f_{app} suffers from substantial chance-projection pairs is evident by f_{tot} decreasing at a faster rate during $t \lesssim 1$ Myr.

Binary activity leads to an overall expansion of the cluster and reduction in ambient temperature, i.e. $\sigma_{\text{op,c}}$. The diminished density and velocity dispersion reduce the encounter rate and rate of binary destruction. Effectively, the binary hardness boundary shifts to longer periods, making further binary-system ionising events less probable because the period distribution has been truncated below the shifting boundary, as discussed in the previous subsection. At $t \approx 5$ Myr, $f_{\text{tot}}^{\text{A1}} = 0.34$ and $f_{\text{tot}}^{\text{A2}} = 0.30$, and the surviving binary population is sufficiently hard that further decrease will not be significant. In the cluster, the binary proportion will increase during the subsequent cluster life-time owing to mass segregation and loss of preferentially single stars (fig. 3 in Kroupa 1995c).

During the first 2 Myr, long-period binary systems are ionised, leading to a period distribution, f_P , that is truncated at progressively shorter periods. Fig. 4 demonstrates that most destruction of long-period ($P > 10^6$ days) binaries occurs within $t \lesssim 0.4$ Myr. There is no significant difference between the period distributions measured within $R \leq 0.5$ pc and $R \leq 1$ pc. Also, the figure shows that the period distributions in models A1 and A2 are similarly truncated by $t \gtrsim 0.4$ Myr. However, in model A1 a somewhat larger proportion of binary systems with $10^5 < P < 10^7$ days remains than in model A2. This is a result of the complex interplay between (i) the cross section for binary-destruction being proportional to σ^{-2} (eqn. 26 in Heggie & Aarseth 1992) with the velocity dispersion σ being larger in model A1 for $1 < t < 5$ Myr, (ii) the binary destruction rate being proportional to the square of the density of binaries (eqn. 26 in Heggie & Aarseth 1992), and (iii) the initially larger binary proportion in model A1.

As is evident from Fig. 5, initially there are fewer binaries near the centre in model A1. This is a

result of immediate disruption of long-period systems from crowding (Section 3.3). Note that most of the cluster is initially confined to $r \lesssim 0.6$ pc ($\log_{10} r \lesssim -0.22$), so that there is no significant difference in the period distributions sampled within $r \leq 0.5$ pc and $r \leq 1$ pc. At $t = 0.2$ Myr, the radial dependence is more pronounced, with binary-star depletion progressing further out, but the outer regions at $r \approx 0.6$ pc retain a high binary proportion. At this stage of cluster evolution, the period distribution is already truncated at $P \approx 10^6$ days within $r \lesssim 0.2$ pc ($\log_{10} r \lesssim -0.70$), but remains roughly primordial at $r \approx 0.6$ pc. Further out, however, f_{tot} drops significantly. These are mostly single stars that have been ejected onto long-period and eccentric orbits in the cluster, and form a transient binary-deficient young halo population. After 1 Myr, there remains a slight radial dependence, with f_{tot} increasing slightly with increasing $r < 1.3$ pc ($\log_{10} r < 0.11$) in model A1. Again, the decay for larger r is a result of primarily low-mass stars being ejected during the disruption of binary systems near the cluster core. The radial dependence has vanished by $t = 5$ Myr due to thorough mixing of the stellar population, and $f_{\text{tot}} \approx 0.34$.

The lower primordial $f_{\text{tot}} = 0.6$, together with the Galactic field Gaussian log-period distribution at birth, leads to no pronounced radial dependence initially in model A2, because most binary systems are too tightly bound to be disrupted through crowding. During times $t \lesssim \text{few} \times t_{\text{cross}}$, i.e. $t \lesssim \text{few} \times 0.06$ Myr, however, f_{tot} is a slightly increasing function of r , until the entire cluster is mixed. A strong decrease in f_{tot} for $r \gtrsim 0.5$ pc ($\log_{10} r \gtrsim -0.30$), and a slight decrease for $r \gtrsim 0.6$ pc are evident at $t = 0.2$ and 1 Myr, respectively, for the same reason as above. However, $f_{\text{tot}} \approx 0.30$ for $t > 1$ Myr and $r \lesssim 10$ pc, and little further evolution is apparent until $t = 5$ Myr.

Unfortunately the observational constraints cannot ascertain that the binary proportion is lower in the central parts (Section 2.3). The uncertainties remain too large. The data can be improved by pushing observational resolution to separations of about 20 AU (0.04 arcsec at a distance of 450 pc) in order to sample the period distribution around its likely maximum at $\log_{10} P \approx 4.5$ [days]. The models show that f_{tot} should be independent of r for $1 < t \lesssim 5$ Myr, by which time the stellar population is well mixed. If observations find evidence for $f_{\text{tot}}(r \approx 1.3 \text{ pc}) > f_{\text{tot}}(r > 1.3 \text{ pc})$ and/or $f_{\text{tot}}(r \approx 1.3 \text{ pc}) > f_{\text{tot}}(r < 0.3 \text{ pc})$ then this would be evidence for a Taurus-Auriga-like f_{P} at birth (model A1), and that the Trapezium Cluster is $t \lesssim 10 t_{\text{cross}}$ old, remembering that the alternative model A2 with a Galactic-field f_{P} does not show significant variations of f_{tot} with r .

5.2. Expanding clusters – B

5.2.1. Cluster evolution

The central density is initially as large as in the equilibrium models, but decreases rapidly (Fig. 6). Noteworthy is the divergence of the two models (B1 with $f_{\text{tot}} = 0.77$ and B2 with $f_{\text{tot}} = 0.48$ initially, see Fig. 1) at $t \approx 0.18$ Myr. Thereafter, model B1, which initially contains more long-period binary systems, evolves with a constant stellar number density in the central region, amounting to $N(R < 0.053 \text{ pc}) \approx 8$ stars. Again, as in the equilibrium models, the break-up of long-period binaries causes cluster cooling, which reduces the velocities and thus aids a part of the expanding cluster to form a bound object. This point will be investigated in more detail in a forthcoming paper. In model B2, which contains fewer long-period binaries, binary cooling is less effective, and a smaller part of the cluster condenses out to form a bound entity. In this case, $N(R < 0.053 \text{ pc}) \approx 2$ stars, the decay being halted after $t \approx 0.4$ Myr.

Noteworthy is that the bound clusters that form in models B1 and B2 still have central densities $\rho_{\text{c}} \approx 10^{4.1}$ and $10^{3.5}$ stars/pc³, respectively. In comparison, the Pleiades Cluster has a central density of

only about 27 systems/pc³ from fig.6 in Raboud & Mermilliod (1998a), or between 14 and 27 systems/pc³ from Pinfield, Jameson & Hodgkin (1998) if the mean stellar mass is 1 M_{\odot} or 0.5 M_{\odot} , respectively.

The projected velocity dispersion within $r < 0.41$ pc, which is initially an order of magnitude larger than in the equilibrium models, remains equal in both models and decreases rapidly owing to the expansion against the gravitational potential and the loss of fast-moving stars from the measurement region ($r \leq 0.41$ pc). The evolution, shown in Fig. 6, slows appreciably after about 0.2 Myr when only the slow-moving tail of the population remains within the central radius. Correction for the significant radial bulk motion is necessary, leading to a reduction in the estimated velocity dispersion by up to about 0.5 km/s at $t \approx 0.07$ Myr. The initial radial bulk velocity, $\langle v_r \rangle = 0$, because the velocity vectors are distributed isotropically. As time progresses, the fast and slow-moving stars separate out, and a maximum bulk velocity within $r < 0.41$ pc of $\langle v_r \rangle = 2.9$ km/s is reached at $t \approx 0.06$ Myr. The sharp decay thereafter comes from the loss of the fast-moving stars from the measurement region.

The central number density is consistent at the three-sigma level with the observational constraint during the time interval $0.05 \lesssim t \lesssim 0.1$ Myr, while the velocity dispersion, $\sigma_{\text{op,c}}$, is consistent at the three-sigma level with the observed value for $0 \lesssim t \lesssim 0.06$ Myr (Fig. 6). Thus this model could be a reasonable description of reality if about 60 per cent of the mass of the cluster was expelled about 50 thousand years ago, at which time the Trapezium Cluster would have gone into a rapid expansion phase.

However, this age is significantly younger than the age inferred from HR diagram fitting (Section 2.1). If the expanding model is correct then this age difference can be explained by the cluster having spent a few 10^5 yr in an embedded phase prior to the postulated gas-expulsion event $\approx 5 \times 10^4$ yr ago.

5.2.2. The binary stars

Rapid expansion halts the disruption of binary systems at an early stage. This is evident in Fig. 7. From this figure it follows that the model apparent binary proportion is consistent with the observational constraint at the three-sigma level for $t \gtrsim 0.05$ Myr, provided primordial $f_{\text{tot}} = 0.6$. A smaller primordial f_{tot} would lead to earlier agreement. The total binary proportion shows little evolution after $t \approx 0.02$ Myr, being $f_{\text{tot}} = 0.68$ in model B1, and $f_{\text{tot}} = 0.47$ in model B2. The latter value is comparable to the binary proportion of late-type systems in the Galactic field ($f_{\text{tot}} = 0.47$, Kroupa 1995a), suggesting that expanding Trapezium-Cluster-type stellar assemblages could account for the majority of the Galactic field population. This is corroborated by the period distribution (Fig. 8) for $\log_{10} P \lesssim 7$. However, the observed period distribution in the Trapezium Cluster appears to be significantly below that of the Galactic field for $\log_{10} P \approx 7.06 - 8.11$ (Scally, Clarke & McCaughrean 1999), which may imply that the Galactic field is not made of unbound Trapezium-Cluster-type assemblages, unless wide multiple systems form through capture in the expanding flow. For model B1, the period distribution has a surplus of orbits with $10^5 < P < 10^8$ days.

There is a distinguishable difference between the period distributions within $R \leq 0.5$ pc and $R \leq 1$ pc (Fig. 8). The distributions undergo no further evolution after $t \approx 0.5$ Myr, but within 0.5 pc, they are somewhat depleted relative to the distributions obtained for systems within 1 pc. In particular, Petr's (1998) observational constraints are in nice agreement with model B2. This depletion results from the dynamical interactions within the remaining low-mass cluster, which has a three-dimensional velocity dispersion of $\sqrt{3} \sigma_{\text{op,c}} \approx 0.35$ pc/Myr (Fig. 6). The time-scale for population mixing within 1 pc is thus roughly 3 Myr.

In model B1, formally with primordial $f_{\text{tot}} = 1$, the total binary proportion increases with projected radius initially (Fig. 9), which is a result of disruptive crowding as in model A1. A slight remaining increase with r is maintained at later times because the stellar population cannot mix as the cluster expands. As in model A2, there is initially no significant radial dependence of f_{tot} in model B2. This is retained at $t = 0.064$ Myr owing to the rapid expansion, and is consistent with the presently available observational constraints suggesting no significant radial dependence within $r \approx 0.3$ pc ($\log_{10} r \approx -0.52$). At $t = 0.2$ Myr, however, both models show a slightly smaller f_{tot} for $r \lesssim 0.16$ pc ($\log_{10} r \lesssim -0.80$) than at larger radii, reflecting the difference in f_{P} for $R \leq 0.50$ pc and $R \leq 1$ pc noted above.

5.3. Clusters in cold collapse – C

5.3.1. Cluster evolution

Cold collapse from an initial Plummer density distribution leads to a rapid increase of the central number density, which is maximised at the cold-collapse (or dynamical) time $t_{\text{cc}} \approx 0.4$ Myr for model C1 ($R_{0.5} = 0.4$ pc initially) and at $t_{\text{cc}} \approx 1.3$ Myr for model C2 ($R_{0.5} = 0.8$ pc initially). Model C2 does not achieve as large a central density as model C1 because the inner regions virialise before the outer regions have fallen in. The evolution is shown in Fig. 10.

The velocity dispersion increases and achieves a maximum at t_{cc} when the clusters rapidly evolve into new equilibrium states through violent relaxation (Lynden-Bell 1967). The projected bulk radial velocity, $\langle v_r \rangle$, decreases as infall progresses. For model C1 the maximum radial bulk motion $\langle v_r \rangle = -0.8$ km/s, and for model C2 it is -0.5 km/s (Fig. 10). The corrections to the projected velocity dispersion are, however, small.

After virialisation, the clusters evolve on the much longer relaxation time-scale. It is longer for virialised model C2, which has a smaller peak density, and consequently the decay of the central density proceeds at a slower rate. In both models, the central density remains significantly larger within 5 Myr than the observational constraint, with an exception only for a short moment at $t \approx 0.06$ Myr for model C2, when the central density briefly passes through the observational constraint. However, the velocity dispersion remains significantly smaller than the observational constraint at all times.

5.3.2. The binary stars

Both models C1 and C2 are assumed to have, formally, a primordial binary proportion $f_{\text{tot}} = 1$. In practice the initial f_{tot} is slightly smaller than 1 (Fig. 1) because of immediate disruption of wide systems through crowding, as in the models above.

At $t = t_{\text{cc}}$, model C1 has a central density and velocity dispersion comparable to the initial ($t = 0$) values in model A1 (Section 5.1.1). The binary population is thus expected to evolve similarly as in model A1, keeping in mind that it has already undergone some evolution during the collapse. This is confirmed by comparing Figs. 11 and 3: the observer deduces similar apparent binary proportions, with the evolution in cluster C1 lagging behind that in cluster A1 by approximately t_{cc} . The slightly higher apparent and total binary proportion in model C1 comes about because the global density remains lower, despite the central density achieving a value close to the initial central density in the equilibrium model A1, and because the velocity dispersion remains lower (see also the discussion of binary disruption in Section 5.1.2).

In model C2 the density does not increase to as high a value as in model C1, so that fewer binary systems are ionised. This leads to an apparent binary proportion that is larger than the observational constraints at all times (upper panel in Fig. 11). During the initial collapse phase, the apparent binary proportion increases slightly due to the increased number of chance projection pairs.

The period distribution, f_P , at different times and different radii in the cluster is shown in Fig. 12. By $t = 1.3$ Myr model C1 has already virialised and mixed, and there is no subsequent radial nor any time variation of f_P . The evolution of f_P through cold collapse is, however, evident in model C2. At $t = 1.3$ Myr, the collapse has arrived at the maximum central density, and f_P is already depleted at long periods. There is a larger depletion of f_P in the more concentrated inner region ($R \leq 0.5$ pc). At $t = 5$ Myr, the cluster is virialised, and f_P is even more depleted at long-periods. The maximum three-dimensional velocity dispersion is $\sigma = \sqrt{3}\sigma_{\text{op,c}} = 2.8$ km/s for model C1, and $\sigma = 2.1$ km/s for model C2 (Fig. 10). Taking these values for the circular orbital velocity of a binary system with a mass of $1 M_\odot$, orbital periods of $10^{5.6}$ days and $10^{6.0}$ days, respectively, are obtained. These values reflect the cutoff periods evident in Fig. 12, and demonstrate the dependence of the rate of disruption of binary systems on the ambient velocity dispersion in a self-gravitating stellar system.

How cold collapse influences the radial distribution of binary systems is shown in Fig. 13. Initially $f_{\text{tot}} \approx 1$ for all r . After one overall free-fall time, $t = t_{\text{cc}} \approx 1.3$ Myr for model C2, the binary proportion is reduced to 60 per cent within $r \approx 0.25$ pc ($\log_{10}r \approx -0.60$), where most of the action during virialisation occurs. At larger radii, f_{tot} increases with r and remains essentially unaffected for $r > 1$ pc, i.e. in regions of the cluster that have not yet fallen in. At $t = 5$ Myr, however, the entire cluster has virialised, and the binary proportion is reduced at all radii, with a remaining slight increase towards the outermost less dense regions of the cluster reflecting some remaining incomplete mixing of the population. In model C1 the collapse time-scale is much shorter (≈ 0.4 Myr), even for the outermost radii, so that the binary proportion is reduced at all radii by $t = 1.3$ Myr. At this time, f_{tot} increases slightly with r for $r \lesssim 0.8$ pc ($\log_{10}r \lesssim -0.10$). This comes about because the cluster is still not completely mixed.

During the violent relaxation phase binary systems are ionised at a larger rate owing to the increased number density. Some of the liberated low-mass stars are ejected to larger radii, leading to the significant drop in f_{tot} at $r \gtrsim 2.5$ pc ($\log_{10}r \gtrsim 0.40$, compare with model A1 in Fig. 5). Such a decrease is not evident very well in model C2 because fewer binary systems are ionised in the less-concentrated core, providing fewer single stars to the outer cluster radii. A slight drop is, however, visible at $r > 3$ pc ($\log_{10}r > 0.48$) in model C2.

By $t = 5$ Myr the binary proportion is larger in the centre of model C1 than at larger radii. This is a result of dynamical mass segregation, and is observed in other young clusters (e.g. Elson et al. 1998; Raboud & Mermilliod 1998b).

6. DISCUSSION

Six different models of the Trapezium Cluster, summarised in Table 1, are evolved using Aarseth’s NBODY5 code. They are clusters in virial equilibrium, expanding clusters assuming a star formation efficiency of 42 per cent and instant gas expulsion, and clusters in cold collapse, assuming the stars freeze out of the molecular cloud with a small relative velocity dispersion. We confront the evolving model population with observational constraints to infer if and how binary properties vary with star-forming conditions, and if the present and past dynamical state of the Trapezium Cluster can be inferred.

The virial equilibrium (A1 and A2) and initially collapsing (C1 and C2) models have, in comparison with the Trapezium Cluster, at all times too high a central number density, while simultaneously having too small a velocity dispersion. These are thus excluded as realistic stellar-dynamical models of the Trapezium Cluster. However, we find that one of the expanding models is a solution that meets the observational constraints (Section 6.4 below).

6.1. Variation of binary proportion with radius

All models show that the variation of the binary proportion with radius, $f_{\text{tot}}(r, t > 0)$, is a diagnostic of the dynamical state of a cluster (Figs. 5, 9 and 13).

For example, if the binary proportion near the centre of the cluster is lower than in its outer regions, then this indicates that the cluster is younger than a few crossing times. If the binary proportion is constant throughout most of the cluster but lower in its outermost regions, then this implies that the cluster is old enough for the stellar population to be well mixed, but young enough for binary activity in the inner regions to have ejected single stars into a halo, i.e. it is a few to ten crossing times old. If the binary proportion near the cluster centre is larger than at larger radii, then this indicates that the cluster is sufficiently old for dynamical mass segregation to have had time to occur.

In particular, the collapsing models demonstrate how binary-destruction propagates to larger radii as collapse progresses, with a well-developed radial dependence of f_{tot} that is to a large extent eradicated after a few crossing times through mixing of the stellar population.

6.2. Evolution of the binary proportion

Despite not being possible solutions, the equilibrium and collapsing models shed important insights on the evolution of the binary population during the first few Myr of a cluster’s lifetime after gas dispersal (Figs. 3, 7 and 11).

The calculations show that binary destruction is very efficient in a dense star cluster. The binary proportion decreases from its initial high value to less than 40 per cent within 1–2 Myr in our virial equilibrium cluster model, with most destruction happening within the first 0.5 Myr. Ultimately, expansion of the cluster shifts the hard/soft binary boundary to longer periods that have already been depleted, thus halting further reduction of the binary population, and reducing the cluster expansion rate. An equilibrium is reached between the global properties of the cluster and its remaining binary population after about 2 Myr.

This implies that the distribution of binary-star periods, in particular the truncation period, in a Galactic cluster is a measure of its dynamical state at birth, or at the moment of maximum compression (e.g. after a cold collapse).

6.3. Binary cooling

The effects of binary activity on the evolution of the central density and velocity dispersion are clearly noticeable in the equilibrium models (Fig. 2).

A large proportion of binaries near the hard/soft interface immediately causes overall cluster expansion, because their activity liberates kinetic energy. This stands in contrast to the immediate onset of core contraction for a single-star cluster.

However, an initially larger proportion of soft binaries (model A1) leads to a cooling effect, because kinetic energy is used up in ionising these binary systems. As a result, the cluster expands at a slower rate, and the central number density remains higher than in model A2 in which there are fewer such primordial binaries. The ratio of the number of binaries with periods near the hard/soft boundary to the number of soft binaries is thus a critical quantity driving the initial rate of expansion.

6.4. A 50 000 yr old Trapezium Cluster?

The expanding models (B1 and B2) are consistent with the observational constraints, provided expansion began $t_{\text{exp}} \approx 5 \times 10^4$ yr ago. This might be possible if about 60 per cent of the mass in the cluster was expelled at that time. Owing to the rapid expansion of models B1 and B2, the initial binary population remains essentially unchanged.

In these models, the binary proportion at a time t_{exp} ago must have been $f_{\text{tot}} \approx 0.48$ to be consistent with the observational constraints. This is lower than the binary proportion in Taurus–Auriga, and, if model B2 does represent reality, may be due to dynamical evolution in the embedded cluster prior to gas expulsion, or due to a dependency on cloud temperature as suggested by Durisen & Sterzik (1994). This would support the assertion that most Galactic-field stars stem from Trapezium-Cluster like assemblages, provided the discrepancy in the proportion of wide binaries in the Trapezium Cluster and the Galactic field can be accounted for (Section 5.2.2).

The finding that expanding model B2 is consistent with the observational constraints suggests that a gas mass of approximately $1000 M_{\odot}$ may have been expelled about 5×10^4 yr ago. This quantity of ejected gas is consistent with observations of outflows from young OB stars (Churchwell 1997). The observations show that hundreds of M_{\odot} of gas are expelled within a few to tens of 10^4 yr per massive star. Our assumption of instantaneous mass loss is thus reasonable. A neutral gas lid lies in front of the Trapezium Cluster as viewed from Earth, but material is streaming out of the blister SW of θ^1 Ori C, where lid extinction is low and vanishes (O’Dell & Wen 1992; Wilson et al. 1997; O’Dell 1999). It is feasible that the massive outflows from the OB stars, that must have existed in the past, escaped from the cluster in that direction.

The possible rather short expansion age of the Trapezium Cluster is interesting in the context of the existence of circum-stellar material around many of the low-mass stars in the Trapezium Cluster. The irradiation by the most massive star in the cluster, θ^1 Ori C, poses a very destructive environment for these objects. Bally et al. (1998) model their photo-evaporation, and find that the ablation is so rapid, that the photo-ionization age of the blister in which the Trapezium Cluster is located may be as short as 10^4 yr. If the age were a few 10^5 yr, most of the circum-stellar material seen around the majority of low-mass stars should have been removed. O’Dell (1999), however, points out that the circum-stellar material may have quasi-equilibrium atmospheres with a much lower mass-loss rate, implying that these objects could be as old as HR diagram fitting implies the cluster to be (Section 2.1).

At present the issue is unsettled, and the present stellar-dynamical models add tantalising evidence in favour of the Trapezium Cluster becoming visible only a few 10^4 yr ago by θ^1 Ori C “turning on”.

6.5. Caveats

The main shortcoming of the present study is that the Trapezium Cluster is treated as an isolated entity. In reality, it appears to be the core of the much more massive and extended Orion Nebula Cluster (ONC). Also, the ONC is partially embedded in the parent elongated molecular gas cloud, the remaining parts of which lie at least about 0.2 pc behind the most massive Trapezium Cluster star, θ^1 Ori C (Wen & O’Dell 1995). Hillenbrand & Hartmann (1998) estimate that the mass in the stellar component of the ONC and in the gas may together suffice to produce the observed stellar velocity dispersion.

It is clear that future models will need to include the ONC, and at a later stage the molecular cloud, being computationally much more expensive. However, even in this context and given the present results, it can be envisioned that the dense core of the ONC, namely the Trapezium Cluster, may have begun expanding a few 10^4 yr ago.

A companion paper (Kroupa 1999) generalises the present results to different values of N and $R_{0.5}$, thereby identifying the candidate sets of models consistent with the observational constraints, if the ONC is in virial equilibrium, expanding or undergoing a cold collapse.

Finally, the results presented here assume the clusters are initially Plummer density distributions. This is realistic in the sense that star-forming cores are centrally concentrated, which has been used in the past to argue that Plummer distributions are reasonable initial conditions for young star clusters (Lada, Margulis & Dearborn 1984). We expect all density distributions that are centrally peaked and that have the same central densities, masses and half-mass radii as the models here to lead to a very similar evolution of the binary population, although the detailed radial dependence at some time t may be slightly different. The greatest differences are expected for clusters that initially consist of groupings of aggregates, in the sense of a hierarchical structure. N-body calculations of the evolution of a cluster of sub-clusters, each containing approximately a dozen binary systems, have to be performed in order to address this particular set of possible models of the Trapezium Cluster and the ONC. However, here again we expect similar evolution in the final bound cluster after the sub-clusters have merged, although the number of escaping stars will be higher during the first few global crossing times (Aarseth & Hills 1972).

7. CONCLUSIONS

This paper presents fully self-consistent stellar-dynamical models of the evolution of the Trapezium Cluster over a time-span of 5 Myr, assuming it consists of 1600 stars with a mass of $700 M_{\odot}$. The calculations treat model clusters that are (i) in virial equilibrium, (ii) expanding and (iii) undergoing cold collapse. All models have a very large primordial binary population. These models constitute the hitherto most realistic stellar-dynamical calculations of a young cluster in existence, covering the time after gas expulsion but before stellar evolution becomes significant. Thus, cooling of a cluster through the ionization of long-period binaries has been discovered for the first time to be a noticeable effect, if the primordial period distribution is similar to what is seen in the Taurus–Auriga star formation complex.

The calculations show that a young compact cluster, that is similar to the Trapezium Cluster and in virial equilibrium, undergoes significant dynamical evolution during the first few Myr. The same holds true for its binary population, which is depleted rapidly, but then stabilises at $f_{\text{tot}} \approx 0.30, 0.34$ if the initial period distribution is as in the Galactic field or Taurus–Auriga-like, respectively. This work also demonstrates which observational constraints are critical for discerning between models of very young

clusters. These are the inner and outer binary proportions, and the radial bulk motion.

In a young cluster the period distribution is truncated at a period that depends on the initial dynamical state of the cluster, with little further evolution after a few Myr, or after violent relaxation has occurred. Measurement of the period distribution, or at least of the truncation period, in a cluster such as the Pleiades or Hyades, thus constrains the possible range of initial configurations of these clusters.

We are particularly interested to have discovered that the expanding cluster model is in best agreement with the observational constraints. This model assumes that about $1000 M_{\odot}$ of gas was expelled from the cluster about 50 000 yr ago, implying that the binary proportion at that time must have been significantly below the Taurus–Auriga value, and that the Trapezium Cluster is unlikely to form a long-lived bound Galactic cluster. The expansion rate is thus a very potent observable that urgently needs to be determined. The present models have a projected bulk radial velocity within a central radius of 0.41 pc of about 2 km/s at an expansion age of 50 000 yr.

While the present models are not a unique set of stellar-dynamical descriptions of the Trapezium Cluster, the present results will form an incentive for future observational studies (i) of the binary proportion in the inner and outer regions of very young star clusters, and (ii) of the velocity dispersion and bulk radial motions in the clusters. The results, and in particular their generalisation to a larger range of parameter space, will also be a strong incentive for conducting further, much more CPU-intensive numerical experiments, which are already being planned and partially underway.

Acknowledgements

We are very grateful to Sverre Aarseth for freely providing NBODY5, and for his unfailing, friendly and uniquely efficient “customer support”. We are also thankful to Bob O’Dell for very useful correspondence, to Tom Megeath and Phil Myers for interesting conversations, and Gijs Nelemans for helpful comments. PK thanks Ron Burman and other staff of the Department of Physics at the University of Western Australia, where part of this paper was written, for their kind hospitality during March 1998, and the staff of the Harvard-Smithsonian Centre for Astrophysics for a very pleasant visit during March–June 1999, where this paper was finished. PK acknowledges support from DFG grant KR1635.

REFERENCES

- Aarseth S.J., 1985, Direct Methods for N-Body Simulations, in Brackbill J.U., Cohen B.I., eds., Multiple Time Scales, Academic Press, London, p.377
- Aarseth S.J., 1994, Direct Methods for N-Body Simulations, in Contopoulos G., Spyrou N.K., Vlahos L., eds., Galactic Dynamics and N-Body Simulations, Springer, Berlin, p.277
- Aarseth S.J., 1999, Cel. Mech. Dyn. Astron., in press (astro-ph/9901069)
- Aarseth S.J., Hills, J.G., 1972, A&A, 21, 255
- Aarseth S.J., Henon M., Wielen R., 1974, A&A, 37, 183
- Bally J., Testi L., Sargent A., Carlstrom J., 1998, AJ, 116, 854

- Bate M.R., Clarke C.J., McCaughrean M.J., 1998, MNRAS, 297, 1163
- Benson P.J., Myers P.C., 1989, ApJS, 71, 89
- Bonnell I.A., Kroupa P., 1999, in McCaughrean M.J., ed., ASP Conf. Ser. Vol.??, The Orion Complex Revisited, Astron. Soc. Pac., San Francisco, in press (astro-ph/9802306)
- Briceno C., Hartmann L., Stauffer J., Martin E., 1998, AJ, 115, 2074
- Churchwell E., 1997, ApJ, 479, L59
- Duchene G., 1999, A&A, 341, 547
- Duquennoy A., Mayor M., 1991, A&A, 248, 485
- Durisen R.H., Sterzik M.F., 1994, A&A, 286, 84
- Elson R.A.W., Sigurdsson S., Davies M., Hurley J., Gilmore G., 1998, MNRAS, 300, 857
- Frink S., Kroupa P., Röser S., 1999, MNRAS, submitted
- Ghez A.M., McCarthy D.W., Patience J.L., Beck T.L., 1997, ApJ, 481, 378
- Gomez M., Hartmann L., Kenyon S.J., Hewett R., 1993, AJ, 105, 1927
- Goodman J., Heggie D.C., Hut P., 1993, ApJ, 415, 715
- Heggie D.C., 1975, MNRAS, 173, 729
- Heggie D.C., Aarseth S.J., 1992, MNRAS, 257, 513
- Hillenbrand L.A., 1997, AJ, 113, 1733
- Hillenbrand L.A., Hartmann L.W., 1998, ApJ, 492, 540
- Jones B.F., Walker M.F., 1988, AJ, 95, 1755
- Köhler R., Leinert Ch., 1998, A&A, 331, 977
- Kroupa P., 1995a, MNRAS, 277, 1491
- Kroupa P., 1995b, MNRAS, 277, 1507
- Kroupa P., 1995c, MNRAS, 277, 1522
- Kroupa P., 1998, MNRAS, 298, 231
- Kroupa P., 1999, NewA, in preparation
- Kroupa P., Tout C.A., Gilmore G., 1993, MNRAS, 262, 545
- Lada C.J., Margulis M., Dearborn D., 1984, ApJ, 285, 141
- Leinert Ch., Zinnecker H., Weitzel N., Christou J., Ridgway S.T., Jameson R., Haas M., Lenzen R., 1993, A&A, 278, 129
- Lynden-Bell D., 1967, MNRAS, 136, 101
- Lynden-Bell D., 1998, in Gervois A., Iagolnitzer D., Moreau M., Pomeau Y., eds., Proceedings of XXth IUPAP International Conference on Statistical Physics, Paris, July 20-24, (cond-mat/9812172)
- Mathieu R.D., 1994, ARA&A, 32, 465
- McCaughrean M.J., Stauffer J.R., 1994, AJ, 108, 1382
- McCaughrean M.J., Rayner J.T., Zinnecker H., Stauffer J.R., 1996, in Beckwith S.V.W., Staude J., Quetz A., Natta A., eds., Disks and Outflows around Young Stars, Lecture Notes in Physics, 465, Heidelberg, Springer, p.33

- Megeath S.T., Herter T., Beichman C., Gautier N., Hester J.J., Rayner J., Shupe D., 1996, *A&A*, 307, 775
- O'Dell C.R., 1999, in McCaughrean M.J., ed., *ASP Conf. Ser. Vol.??, The Orion Complex Revisited*, Astron. Soc. Pac., San Francisco, in press
- O'Dell C.R., Wen Z., 1992, *ApJ*, 387, 229
- Ostriker E.C., 1999, *ApJ*, 513, 252
- Padgett D.L., Strom S.E., Ghez A., 1997, *ApJ*, 477, 705
- Pinfield D.J., Jameson R.F., Hodgkin S.T., 1998, *MNRAS*, 299, 955
- Petr M.G., 1998, *Binary Stars in the Orion Trapezium Cluster: A High angular Resolution Near-Infrared Imaging Study*, PhD thesis, University of Heidelberg
- Petr M.G., Coudé du Foresto V., Beckwith S.V.W., Richichi A., McCaughrean M.J., 1998, *ApJ*, 500, 825
- Prosser C.F., Stauffer J.R., Hartmann L.W., Soderblom D.R., Jones B.F., Werner M.W., McCaughrean M.J., 1994, *ApJ*, 421, 517
- Raboud D., Mermilliod J.-C., 1998a, *A&A*, 329, 101
- Raboud D., Mermilliod J.-C., 1998b, *A&A*, 333, 897
- Richichi A., Leinert Ch., Jameson R., Zinnecker H., 1994, *A&A*, 287, 145
- Saiyadpour A., Deiss B.M., Kegel W.H., 1997, *A&A*, 322, 756
- Scally A., Clarke C., McCaughrean M.J., 1999, *MNRAS*, in press (astro-ph/9902156)
- Scalo J.M., 1986, *Fund. Cosmic Ph.*, 11, 1
- Spurzem R., Takahashi K., 1995, *MNRAS*, 272, 772
- Tian K.P., van Leeuwen F., Zhao J.L., Su C.G., 1996, *A&AS*, 118, 503
- van Altena W.F., Lee J.T., Lee J.-F., Lu P.K., Upgren A.R., 1988, *AJ*, 95, 1744
- Wen Z., O'Dell C.R., 1995, *ApJ*, 438, 784
- Wilson T.L., Filges L., Codella C., Reich W., Reich P., 1997, *A&A*, 327, 1177

1	2	3	4	5	6	7	8	9
Model	$R_{0.5}$ (pc)	$N_{c,sys}$	$N_{c,st}$	$\log_{10}(\rho_c)$ (pc^{-3})	Q	f_{tot}	$\log_{10}P_{max}$ (days)	period distribution
A1	0.10	376	624	5.92	0.50	1.0	8.43	K2
A2	0.10	441	624	5.92	0.50	0.6	11.0	DM91
B1	0.10	376	624	5.92	1.20	1.0	8.43	K2
B2	0.10	441	624	5.92	1.20	0.6	11.0	DM91
C1	0.40	60	120	4.12	0.01	1.0	8.43	K2
C2	0.80	3	6	3.21	0.01	1.0	8.43	K2

Table 1: Initial conditions for Trapezium Cluster models. Three calculations are performed for each model. K2 is Kroupa (1995b), and DM91 is Duquennoy & Mayor (1991)

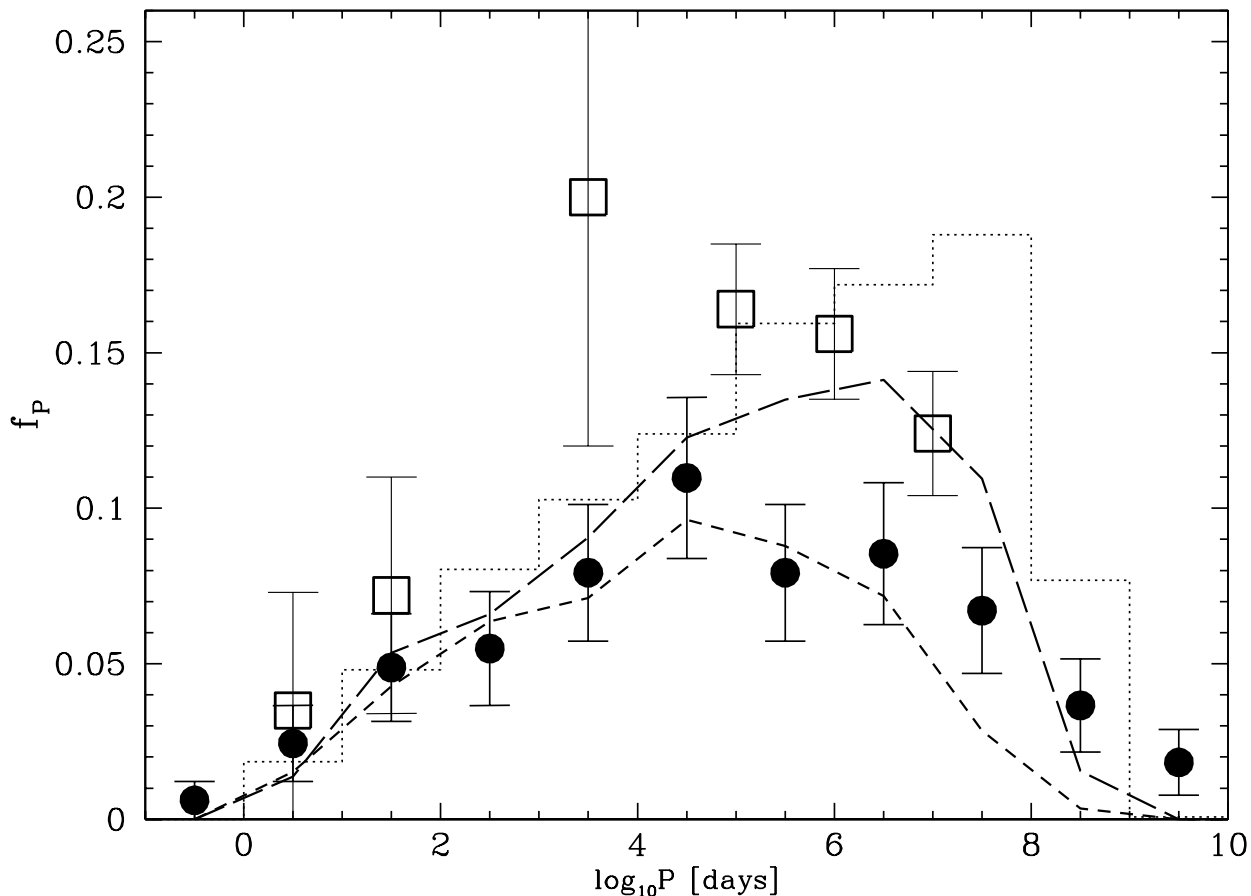


Fig. 1.— Distribution of orbits, f_P , for main sequence multiple systems (solid dots, Duquennoy & Mayor 1991) and pre-main sequence systems in Taurus–Auriga (open squares; $\log_{10} P > 4$: Köhler & Leinert 1998, $\log_{10} P = 3.5$: Richichi et al. 1994, $\log_{10} P < 2$: Mathieu 1994). Main sequence G-, K- and M-dwarf binaries have essentially the same period distribution (fig. 1 in Kroupa 1995a). The observational data include triple systems, which are counted as two orbits. Quadruple systems add three orbits. The dotted histogram is the primordial period distribution from Kroupa (1995b, fig. 7) with $f_{\text{tot}} = 1$. Crowding in Trapezium Cluster models A and B changes this distribution to the initial long-dashed one. Thus, a primordial $f_{\text{tot}} = 1$ becomes $f_{\text{tot}} = 0.77$ initially. A primordial Gaussian log-period distribution with $f_{\text{tot}} = 0.6$ that fits the solid dots, changes in the models to the initial distribution shown as the short-dashed line, with $f_{\text{tot}} = 0.48$. For model A, the initial hard/soft binary boundary (Heggie 1975) is $\log_{10} P_{\text{th}} = 5.4$, which is the orbital period for an orbit with a circular velocity equal to the velocity dispersion in the cluster (three-dimensional velocity dispersion $\sigma = \sqrt{3} \sigma_{\text{op,c}} = 3.46$ km/s, Fig. 2). Systems with $P > P_{\text{th}}$ are *soft*, whereas systems with $P < P_{\text{th}}$ are *hard*.

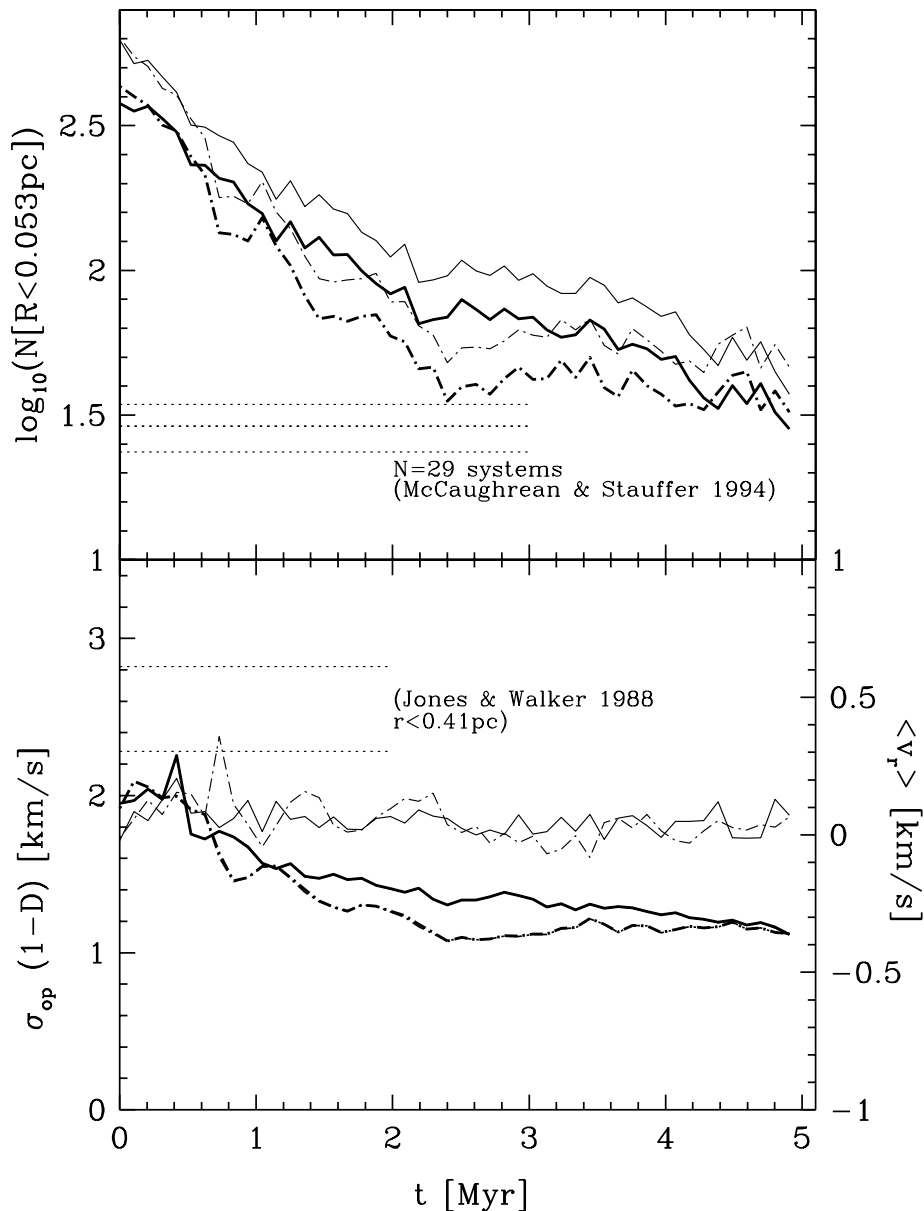


Fig. 2.— Models A1 and A2. In both panels, solid curves are for primordial $f_{\text{tot}} = 1$ (model A1), and dot-dashed curves are for primordial $f_{\text{tot}} = 0.6$ (model A2). Upper panel: Time evolution of the number of stellar systems within a central radius $R = 0.053$ pc. Thick curves assume no binary systems are resolved, and thin curves count all stars. The observational constraint with the Poisson error range is indicated by the dotted lines. Lower panel: Time evolution of the one-dimensional velocity dispersion in the observational plane of centre-of-masses within a projected central radius $r = 0.41$ pc (σ_{op} , thickest curves). Thinnest curves are the projected mean radial velocity within $r = 0.41$ pc ($\langle v_r \rangle$, right ordinate), while the curves with intermediate thickness show the projected velocity dispersion corrected for the radial bulk motion, $\sigma_{\text{op},c}$ (overlapping here with σ_{op}), and are the model quantities to be compared with the observational constraints. The observational one-sigma uncertainty range for $\sigma_{\text{op},c}$ is indicated by the dotted lines. The initial relaxation time for models A1 and A2 is $t_{\text{relax}} = 0.62$ Myr.

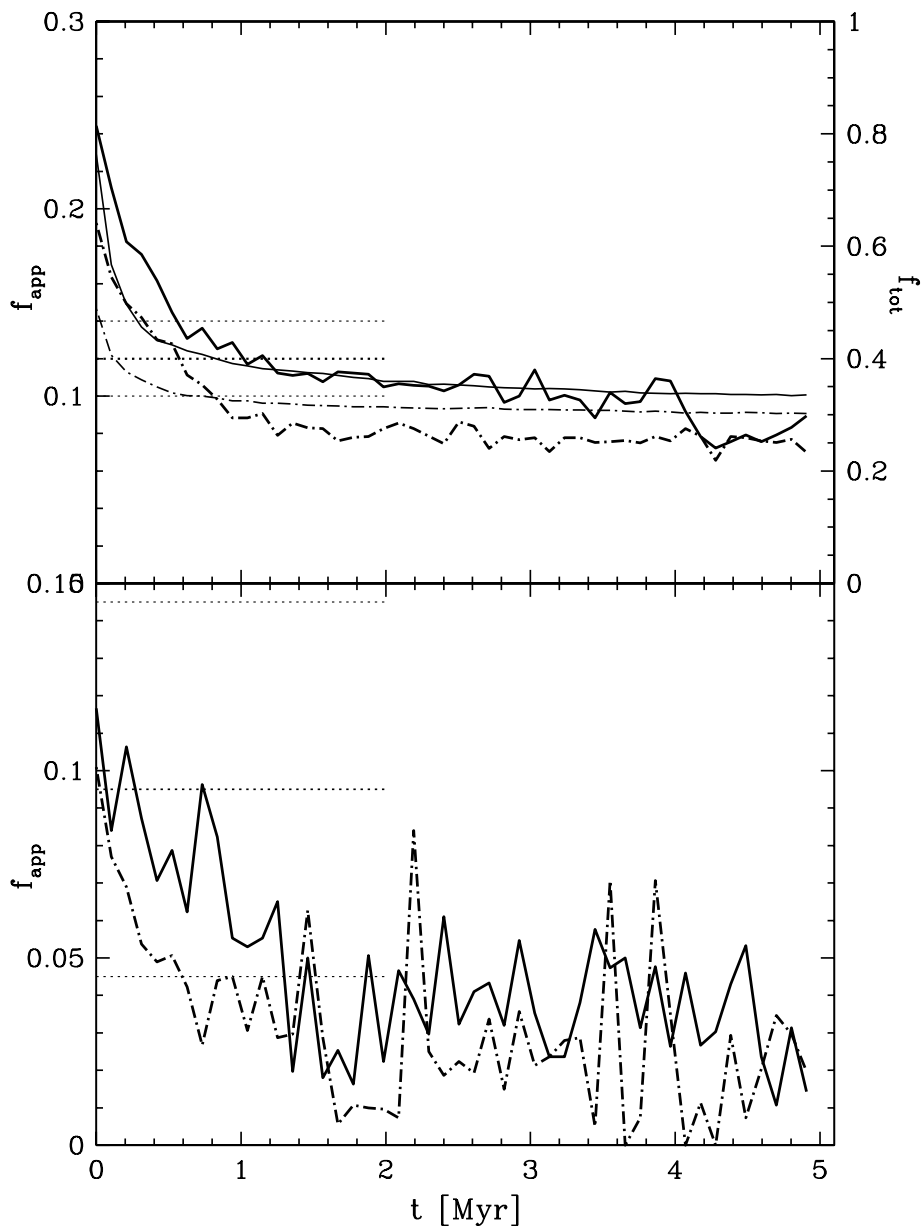


Fig. 3.— Time evolution of the projected apparent binary proportion (thick lines). Solid line is for primordial $f_{\text{tot}} = 1$ (model A1) and dot-dashed line is for primordial $f_{\text{tot}} = 0.6$ (model A2). Upper panel: Observational constraints on f_{app} from Prosser et al. (1994, $r = 0.249$ pc, $d_1 = 26$ AU, $d_2 = 440$ AU, see Section 4.2) are shown as dotted lines. Thin lines are the proportion of all bound binary systems, f_{tot} (right ordinate). Lower panel: Observational constraints from Petr et al. (1998, $r = 0.04$ pc, $d_1 = 63$ AU, $d_2 = 225$ AU) are shown as the horizontal lines. The central dotted line is f_{app} for all systems in their sample, which is to be compared with the theoretical results. Poisson uncertainties are indicated by the upper and lower horizontal lines. For comparison with Fig. 4, a semi-major axis $a = 26$ AU corresponds to an orbital period in days of $\log_{10}P = 4.7$ for a $1 M_{\odot}$ system. Similarly, $a = 440$ AU corresponds to $\log_{10}P = 6.5$, $a = 63$ AU corresponds to $\log_{10}P = 5.3$, and $a = 225$ AU corresponds to $\log_{10}P = 6.1$. The initial crossing time for models A1 and A2 is $t_{\text{cross}} = 0.06$ Myr.

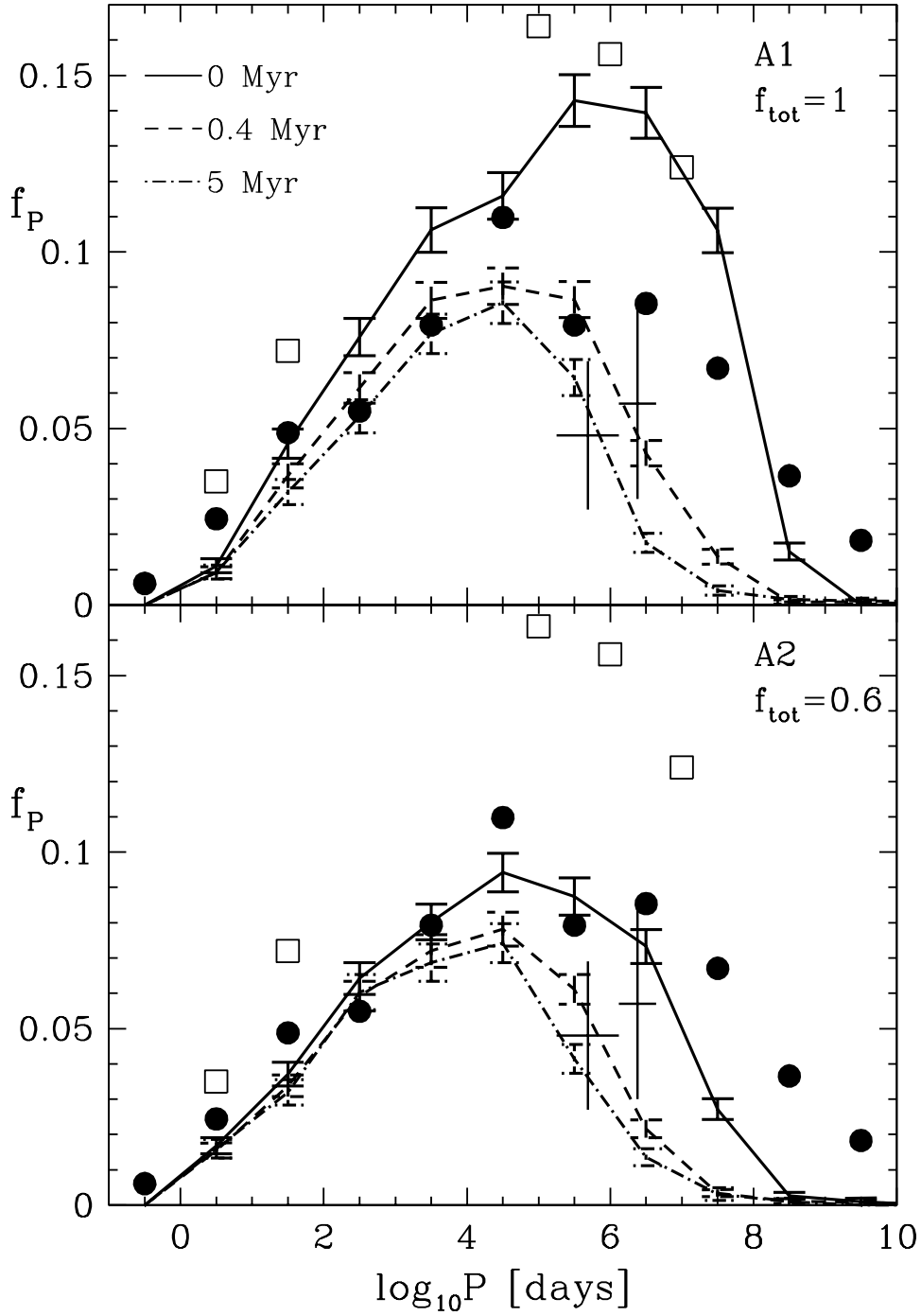


Fig. 4.— Period distribution for all binary systems within $R \leq 1$ pc of the density maximum (higher order systems are not counted). Upper panel and lower panels are for models A1 and A2, respectively. Observational data in both panels are as in Fig. 1. The two large crosses at $\log_{10}P = 5.69$ and $\log_{10}P = 6.38$ are one-sigma observational constraints for $r < 0.3$ pc and $0.07 < r < 0.3$ pc, respectively (Petr 1998).

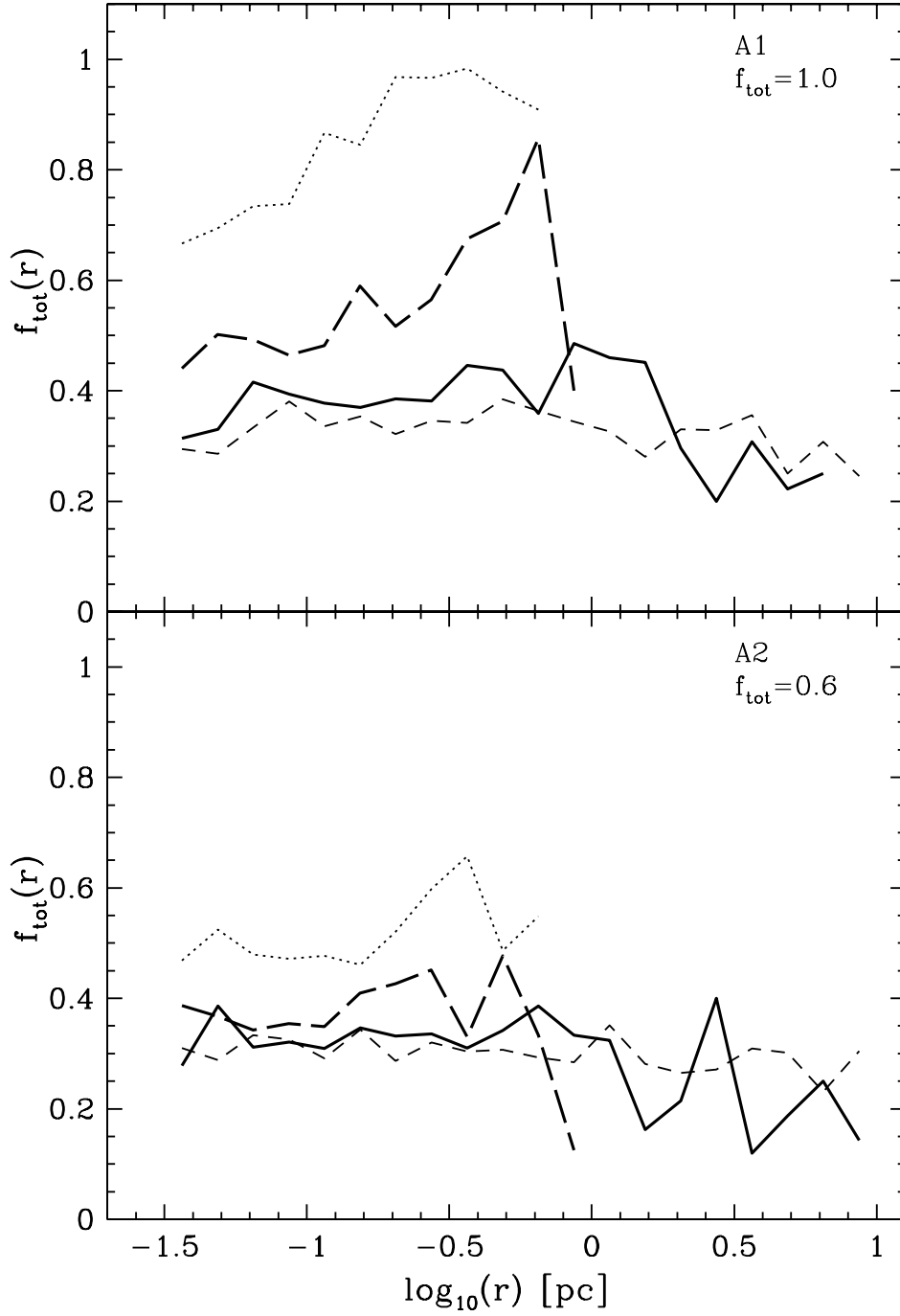


Fig. 5.— Projected radial dependence of the total binary proportion, $f_{\text{tot}}(r)$ (equation 2). In both, the upper (model A1) and the lower panel (model A2), dotted lines are the initial distributions, long-dashed lines are for $t = 0.2$ Myr, solid lines are for $t = 1$ Myr and short-dashed lines are for $t = 5$ Myr.

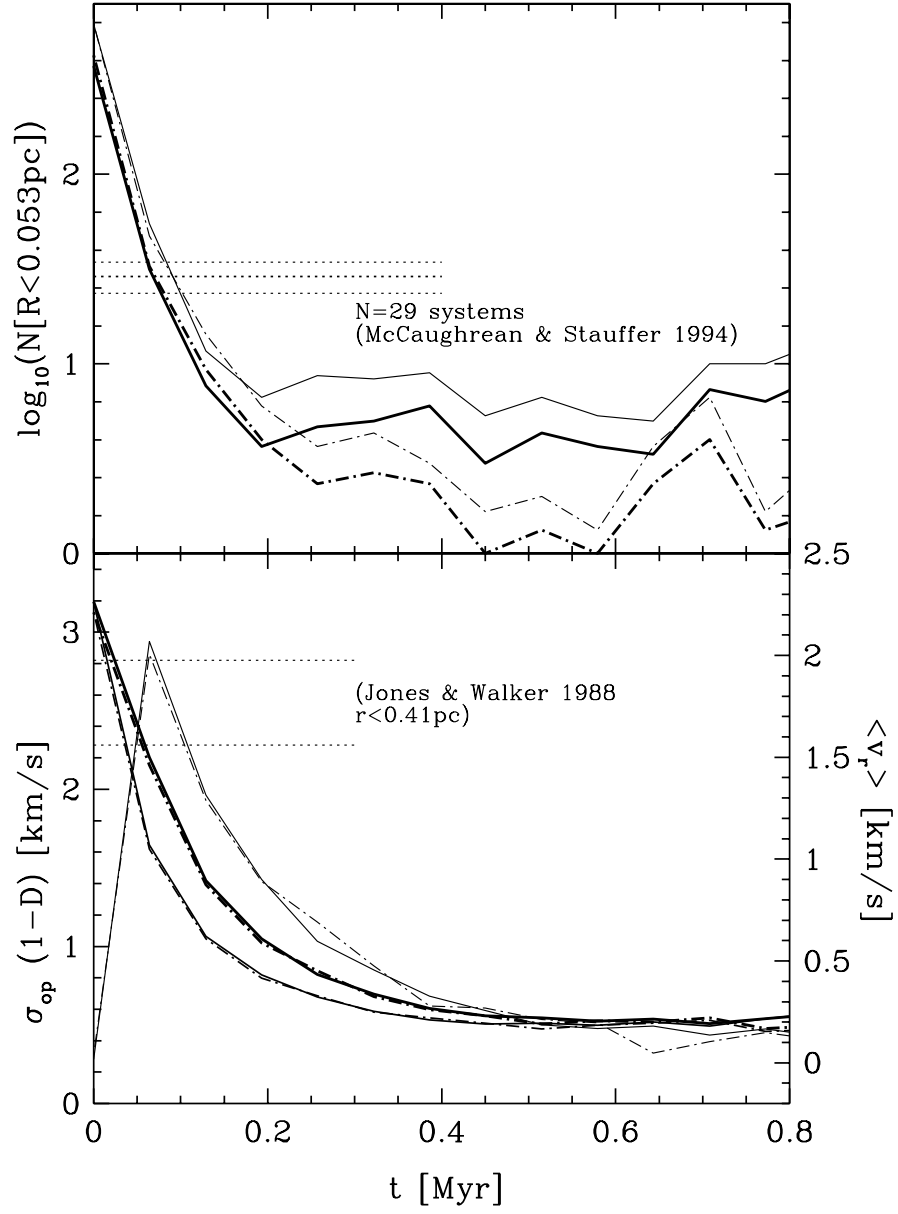


Fig. 6.— As Fig. 2, but for expanding models B1 (solid curves) and B2 (dot-dashed curves).

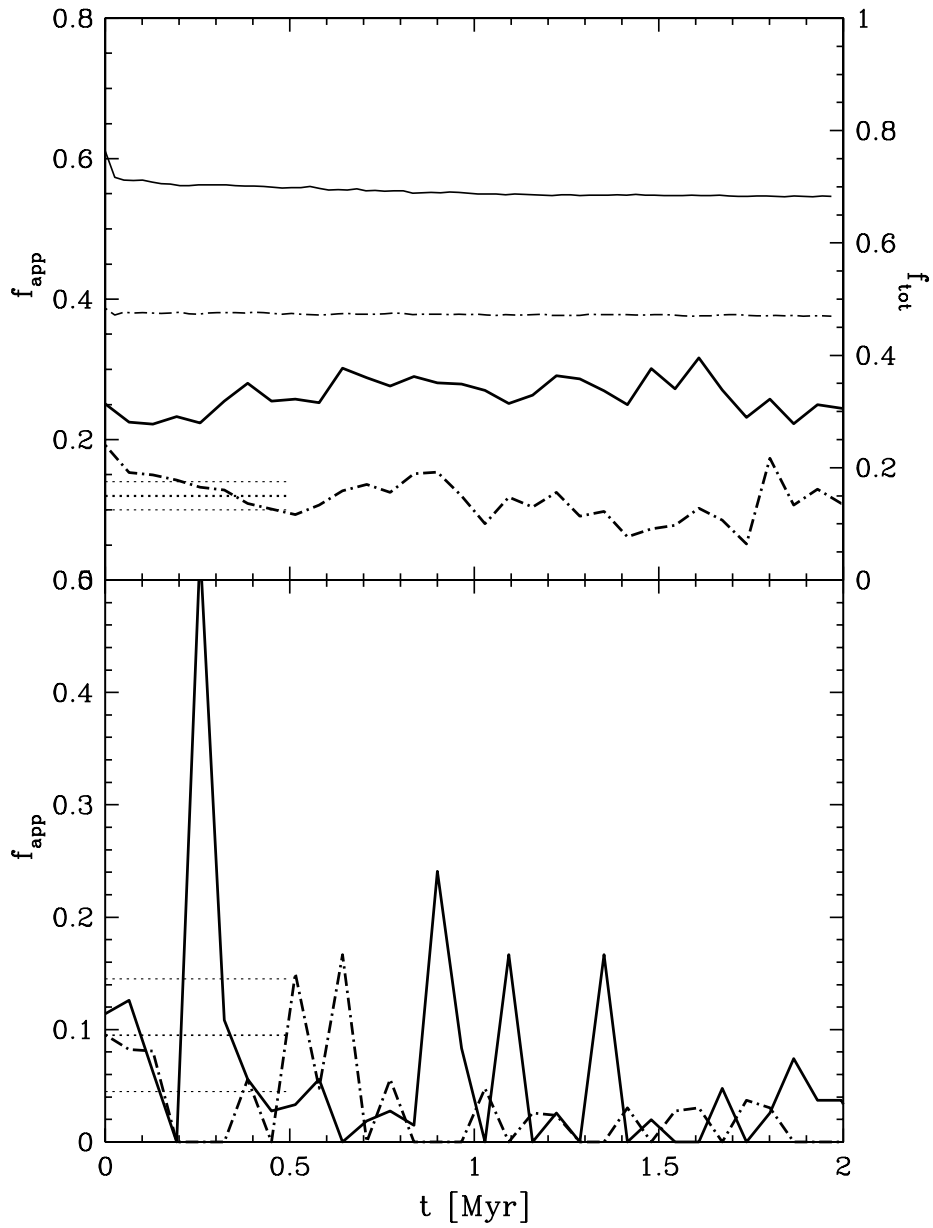


Fig. 7.— As Fig. 3, but for expanding models B1 (solid curve) and B2 (dot-dashed curve).

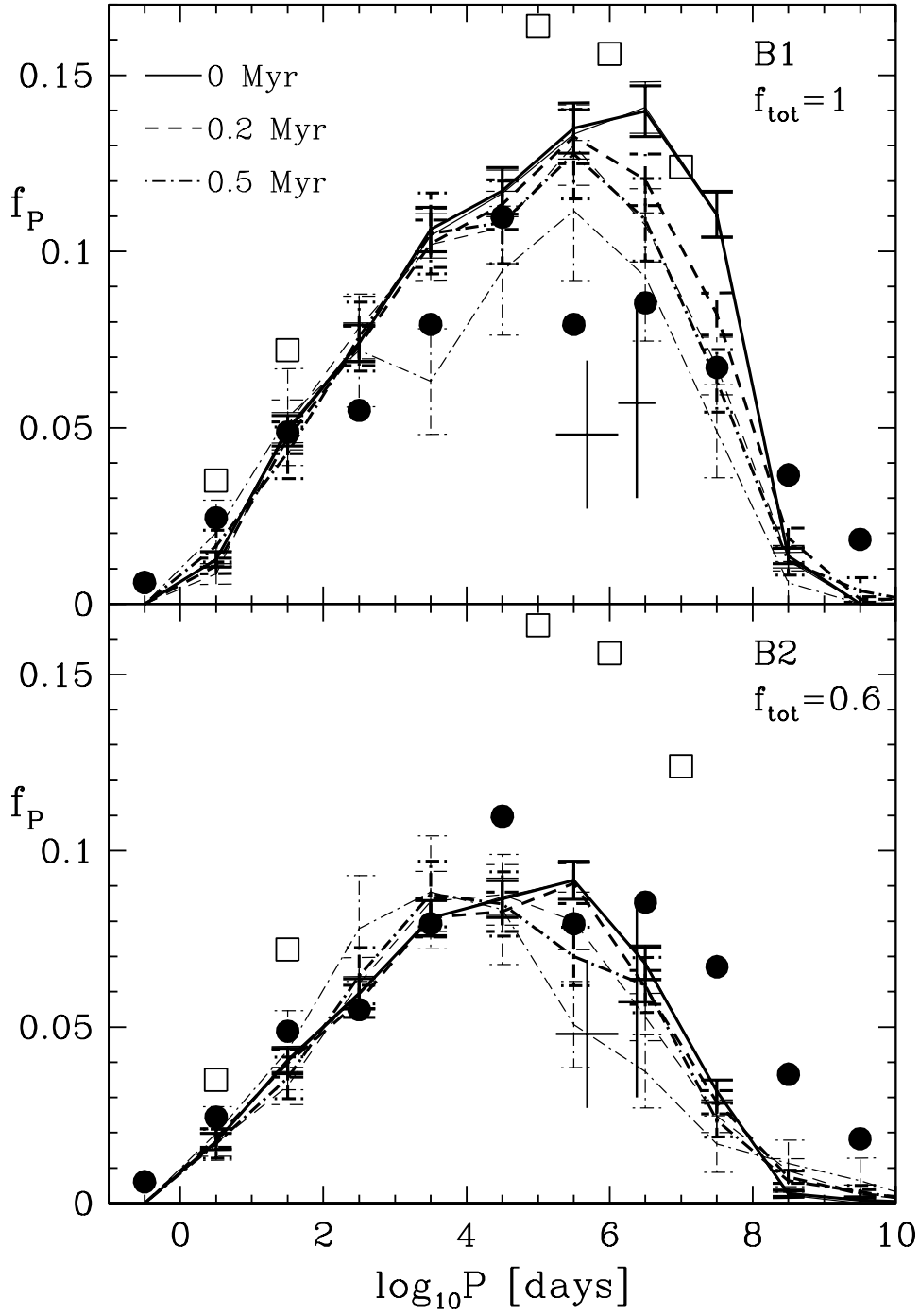


Fig. 8.— As Fig. 4, but for expanding models B1 (upper panel) and B2 (lower panel). Thick and thin curves are for binaries with $R \leq 1$ pc and $R \leq 0.5$ pc, respectively.

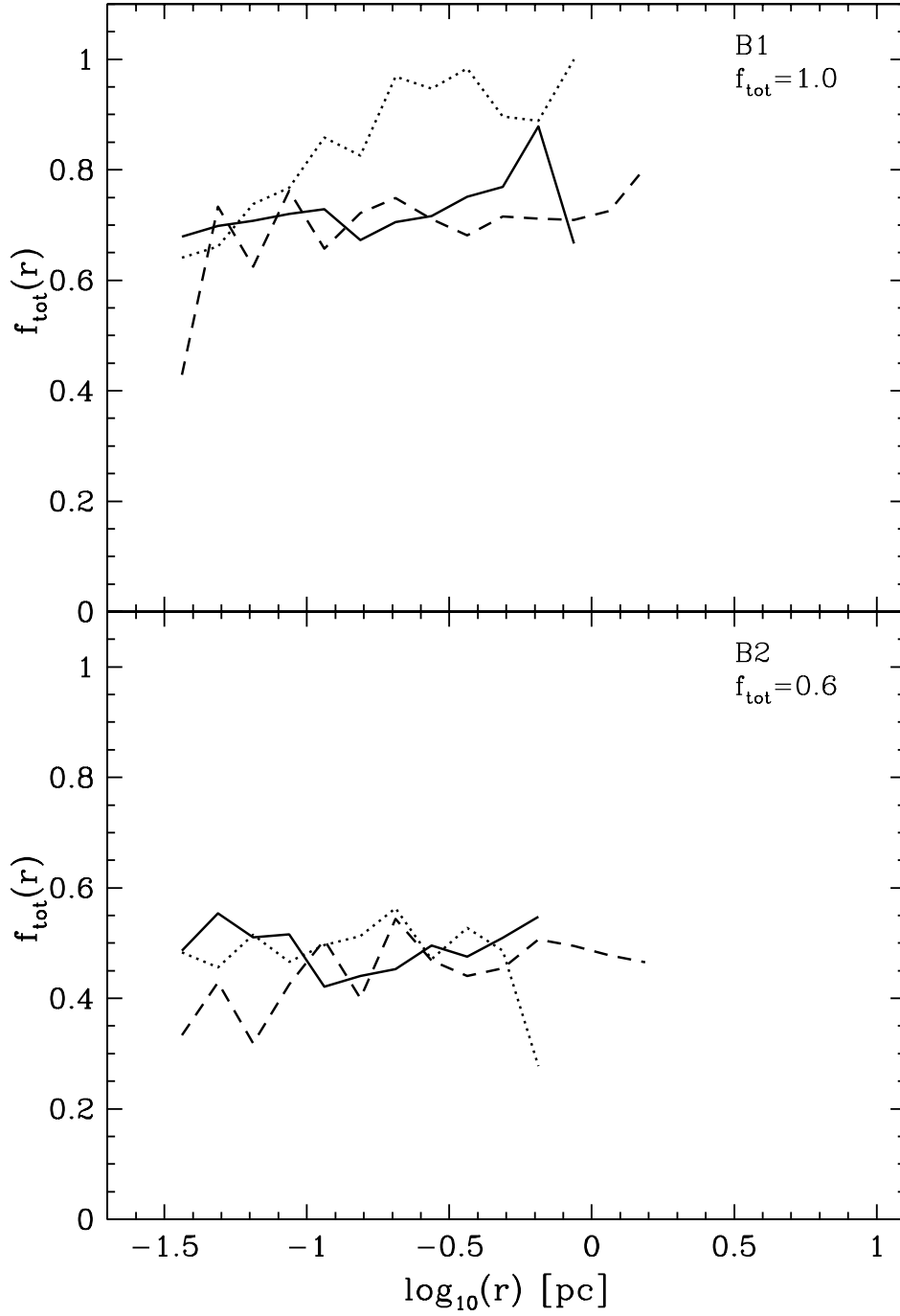


Fig. 9.— As Fig. 5, but for expanding models B1 (upper panel) and B2 (lower panel). In both panels, the dotted line is the initial distribution, and the solid and dashed lines are $f_{\text{tot}}(r)$ at $t = 0.064$ Myr and 0.2 Myr, respectively.

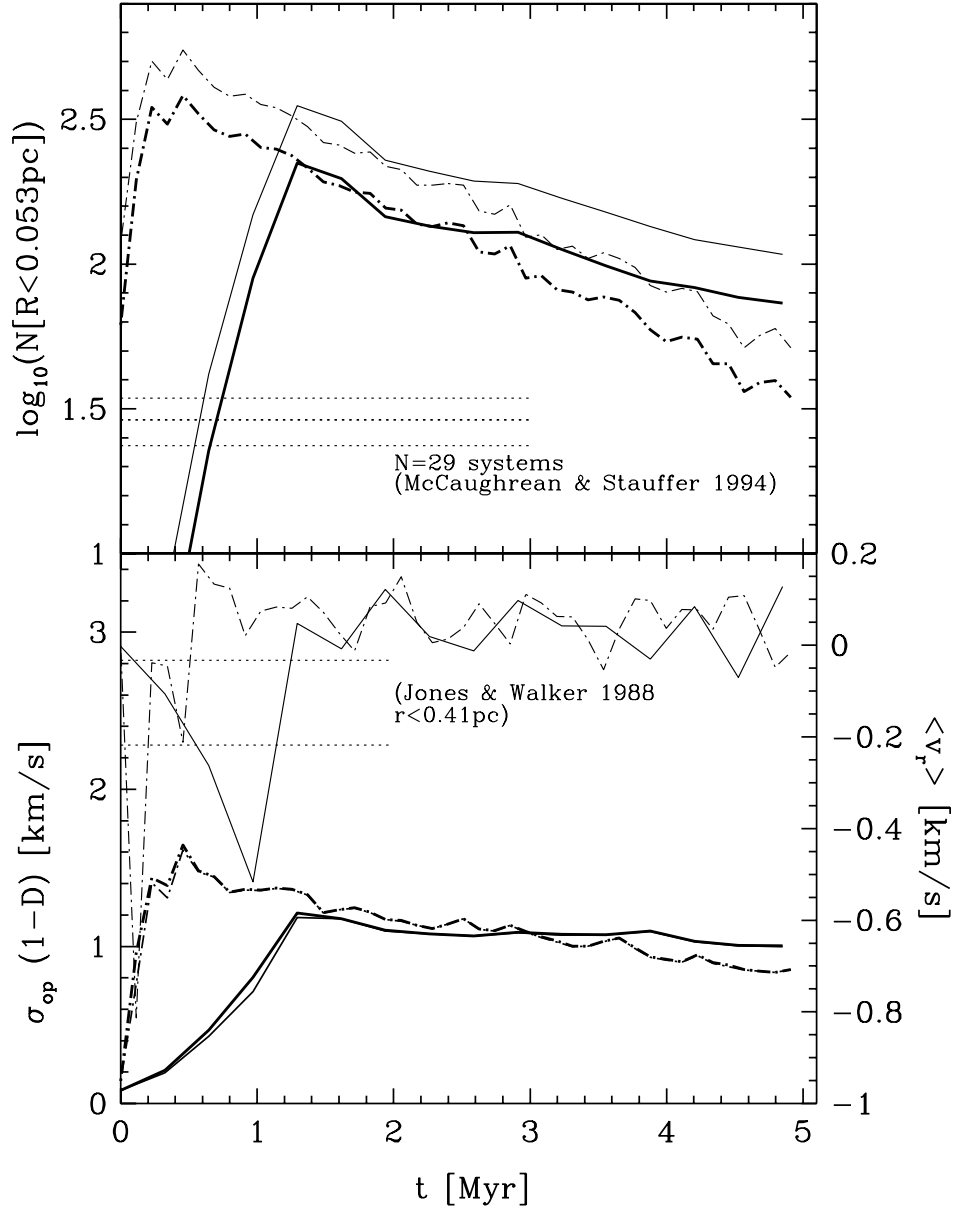


Fig. 10.— As Fig. 2, but for collapsing models C1 (dot-dashed curves) and C2 (solid curves).

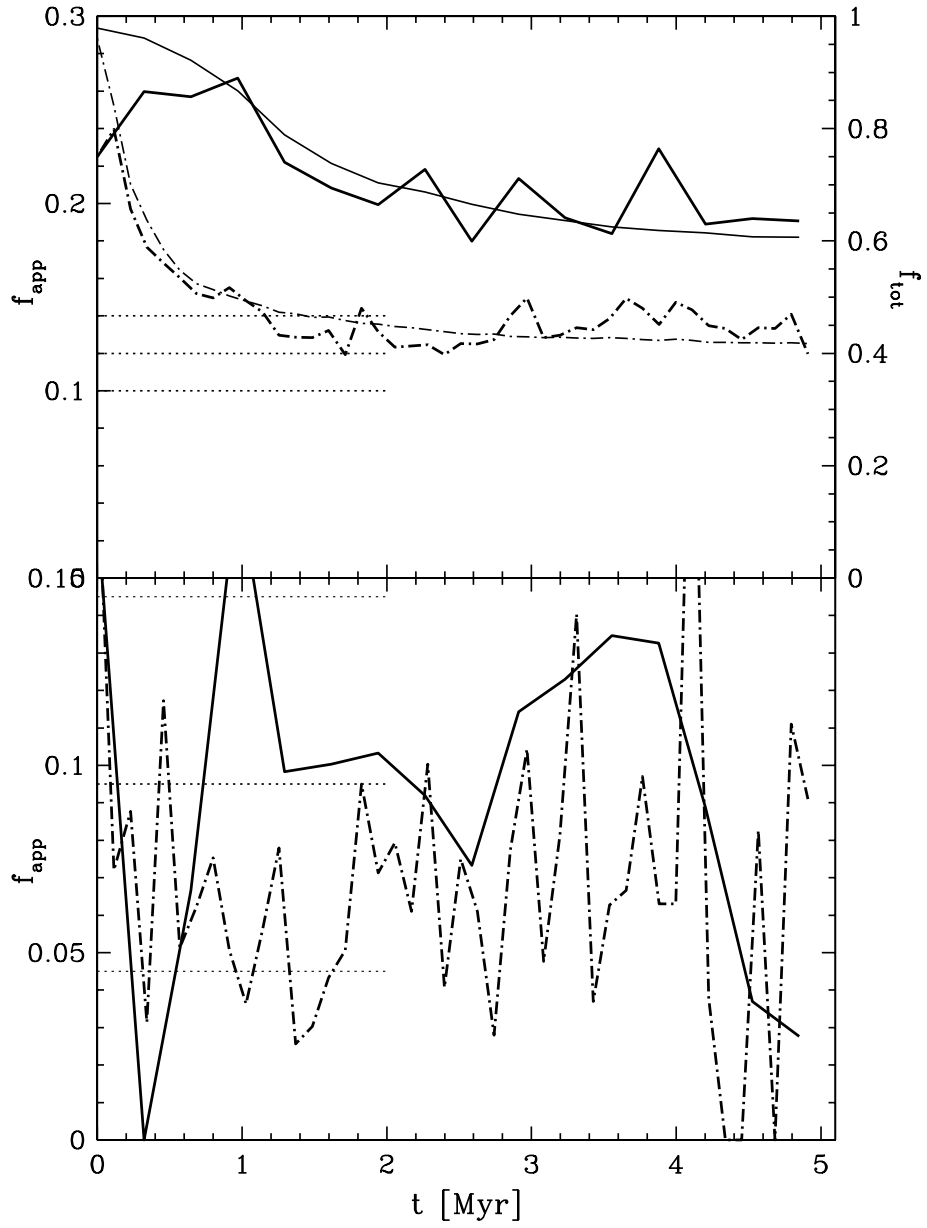


Fig. 11.— As Fig. 3, but for collapsing models C1 (dot-dashed curve) and C2 (solid curve).

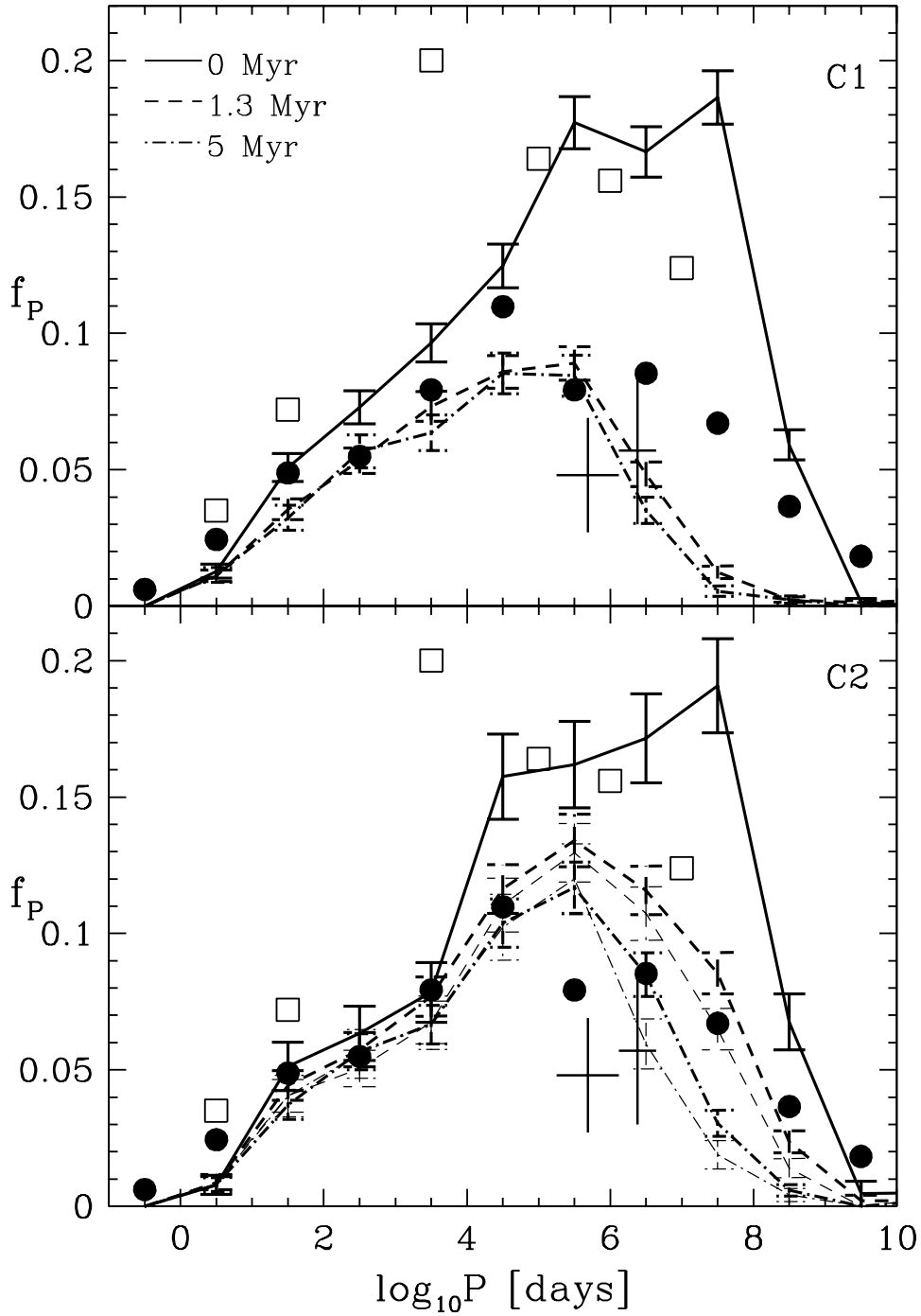


Fig. 12.— As Fig. 4, but for collapsing models C1 (upper panel) and C2 (lower panel). Thick and thin curves are for $R \leq 1$ pc and $R \leq 0.5$ pc, respectively. The distribution for $R \leq 0.5$ pc is only shown in those cases where a significant difference to the $R \leq 1$ pc distribution exists.

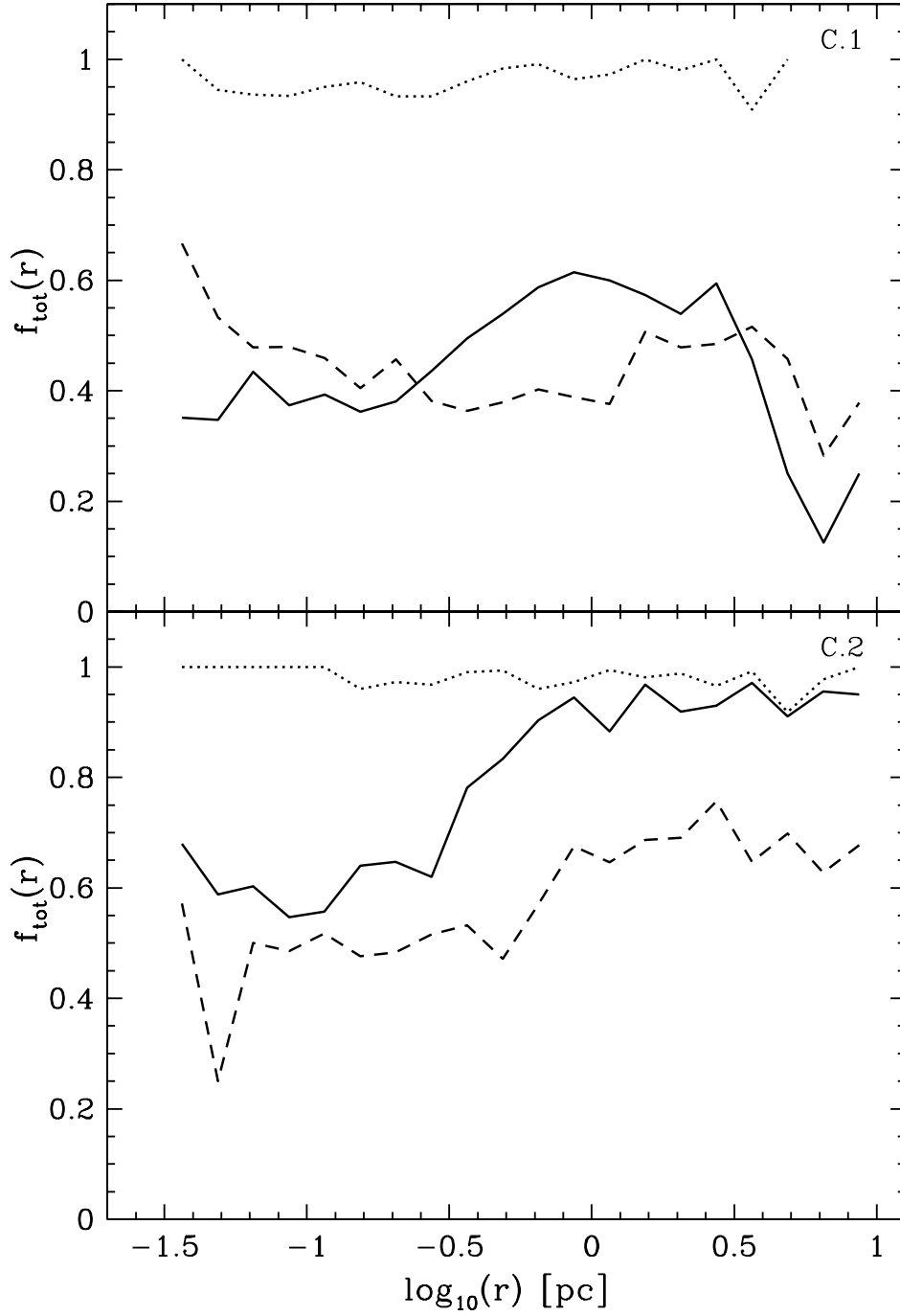


Fig. 13.— As Fig. 5, but for collapsing models C1 (upper panel) and C2 (lower panel). In both panels, the dotted line is the initial distribution, and the solid and dashed lines are $f_{\text{tot}}(r)$ at $t = 1.3$ Myr and 5 Myr, respectively.